The Effect of Salt on a Binary Lyotropic Liquid Crystal System

Farouq Eniola Usman

Submitted to the
Institute of Graduate Studies and Research
in partial fulfillment of the requirements for the degree of

Master of Science
in
Physics

Eastern Mediterranean University
September 2021
Gazimağusa, North Cyprus

Approval of the Institute of Graduate Studies and Research

Prof. Dr. Ali Hakan Ulusoy
Director

I certify that this thesis satisfies all the requirements as a thesis for the degree of Master of Science in Physics.

Prof. Dr. Izzet Sakalli
Chair, Department of Physics

We certify that we have read this thesis and that in our opinion it is fully adequate in scope and quality as a thesis for the degree of Master of Science in Physics.

Asst. Prof. Dr. Mehmet Okcan
Supervisor

Examining Committee

1. Prof. Dr. Ayhan Bilsel

2. Asst. Prof. Dr. Mehmet Okcan

3. Asst. Prof. Dr. Mustafa Riza

ABSTRACT

This study is conducted with the purpose of understanding the effect of inorganic salt (sodium bromide, NaBr) on the phase states, phase behaviour and physical properties of a binary lyotropic liquid crystal system (tetradecyl trimethyl ammonium bromide, TTAB + water). For this purpose, first the phase behaviour, lyotropic and thermotropic phase transitions, of the binary system was investigated and the phase diagram of the binary system was constructed. The refractive index and electrical conductivity values of all the mesophases defined in the binary system were determined in large temperature intervals.

The refractive index – temperature, refractive index – concentration, electroconductivity – temperature and electroconductivity – concentration dependences were graphed analysed and presented. Later, we prepared a solution of ultrapure water and sodium bromide, with $95wt\%$ water and $5wt\%$ NaBr, and used it as solvent, instead of ultrapure water used in binary system, to prepare the samples. We repeated the procedure for the binary system, constructed a phase diagram and investigated the behaviour of physical parameters for this new system.

To understand the effect of salt on the phase behaviour, lyotropic and thermotropic phase transitions and the polymorphism of the binary system the two-phase diagrams were compared, and the results were discussed. Likewise, to understand the effect on physical parameters all the dependences obtained and represented were compared and discussed.

Keywords: Lyotropic liquid crystal, conductivity, refractive index, salt effect

ÖZ

Bu çalışma inorganik tuzun (NaBr) ikili bir liyotropik sıvı kristal sistemin (tetradesil trimetil amoyum bromid, TTAB + su) faz helleri, faz davranışları ve fiziksel özellikleri üzerine olan etkisinin incelenmesi amacı ile yapılmıştır.

Bu amaç Doğrultusunda ilk önce ikili sistemin faz davranışları ile liyotropik ve termotropik faz geçişleri incelenmiş ve ikili sistemin faz diyagramı kurulmuştur. İkili sistemde belirlenen tüm ara fazların kırılma indisi ve elektriksel iletkenlik değerleri geniş sıcaklık aralıklarında belirlenmiştir. Kırılma indisi – sıcaklık, Kırılma indisi – konsantrasyon, elektriksel iletkenlik – sıcaklık ve elektriksel iletkenlik – konsantrasyon bağlılık grafikleri çizilmiş, analiz edilmiş ve sunulmuştur.

Daha sonra, örneklerin hazırlanması için ultra saf su yerine $95\%wt$ ultra saf su ve $5\%wt$ NaBr çözeltisi kullanılmıştır. Yukarıda ikili sistem için anlatılan prosedür kullanılarak bu sistemin de faz diyagramı kurulmuş ve fiziksel parametrelerinin davranışları belirlenmiştir.

Tuzun faz davranışlarına, liyotropik ve termotropik faz geçişlerine ve ikili sistemin polimorfizmine etkisinin anlaşılması için iki faz diyagramı kıyaslanmış ve tartışılmıştır. Benzer şekilde tuzun fiziksel parametreler üzerine etkisinin anlaşılması için de elde edilen ve sunulan tüm bağlılıklar kıyaslanmış ve tartışılmıştır.

Anahtar kelimeler: Liyotropik sıvı kristal, iletkenlik, kırılma indisi, tuz etkisi

ACKNOWLEDGEMENT

First and foremost I will love to thank Allah (SWT) who spared my life up till this moment, made this thesis a sucess for me, and who in his infinite mercy has guided me throughout this phase.

All thanks to my parents Mr and Mrs Usman, my siblings Mubaraq Usman and Mukhtar Usman, who also supported me during this period. They sacrificied so much for me to be able to achieve my goal, I am so grateful to them.

I would love to thank my supervisor Assist. Prof. Dr. Mehmet Ockan, who has guided me from the begining of my thesis up to the end.

I would love to thank my girlfriend also, the person of Zainab Jimoh. She stood by me througout my program with lots of advice and prayers, for that I am grateful.

Also, all thanks to my friends Yussuf Okandeji, Tejiri Otite, Collins Edet, Mahmoud Farouq, Khadijah Abdul Salam, Mariam Abolade, Khadijah Olaitan, Azeemah Owolabi, Mariam Yussuf, Anat Oseni, Walliyah Popoola, Maunah Abdul Malik, Hajarah Aliyu and Muheeza Oke whom they were so good to me from the begining to the end, supporting me with advice and prayers. Am grateful for having you guys as my friend.

TABLE OF CONTENTS

LIST OF TABLES

LIST OF FIGURES

LIST OF SYMBOLS AND ABBREVIATIONS

$\hat{n}$	Director
n	Refractive index
$n = f(T)$	Refractive index – temperature dependence
n_e	Extraordinary refractive index
n_0	Ordinary refractive index
Δn	Difference in refractive index
$n_\perp$	Perpendicular refractive index
$n_\parallel$	Parallel refractive index
θ	Angle between long axis of each molecule and the director
$>$	Greater than
$<$	Less than
$<>$	Average of all molecules in the sample
σ	Conductivity
$\sigma = f(T)$	Conductivity – temperature dependence
ρ	Resistivity
γ	Critical packaging parameter
a_0	Optimum area for the head group
l_c	Critical chain length
BLS	Binary lyotropic system
CMC	Critical micelle concentration
Cpp	Critical packaging parameter
D	Lamellar D

DNA	Deoxyribonucleic acid
E	Hexagonal E
L_1	Isotropic micellar L_1
LC	Liquid crystal
LCD	Liquid crystal display
LLC	Lyotropic liquid crystal
N_{BX}	Nematic biaxial
N_C	Nematic calamitic
N_D	Nematic discotic
NaBr	Sodium bromide
pBLS	Pseudo binary lyotropic system
POM	Polarizing optical microscope/microscopy
RI	Refractive index
RNA	Ribonucleic acid
S	Order parameter
T	Temperature
Tc	Temperature at which LC to liquid phase transition occurs
TLC	Thermotropic liquid crystal
TLS	Ternary lyotropic system
TN	Twisted nematic
TTAB	Tetradecyl trimethyl ammonium bromide
V	Volume of hydrocarbons

Chapter 1

INTRODUCTION

1.1 Historical Background

In 1888, Friedrich Reintizer, an Austrian botanist was investigating a variety of cholesterol derivatives with the aim of understanding their physio-chemical properties. He found that cholesteryl benzoate had a strange melting behaviour. In his study, he noticed that the solid specimen of cholesteryl benzoate he was investigating did not melt directly into a transparent liquid as expected upon heating. Rather, its crystals first melted into a hazy liquid and then into a transparent liquid at a higher temperature, as presented in Figure1.1. Based on repeated observations, Reintizer claimed that the substance has two observable melting points. He also mentioned that the hazy liquid observed after the first melting still had some order contrary to the later formed transparent liquid [1].

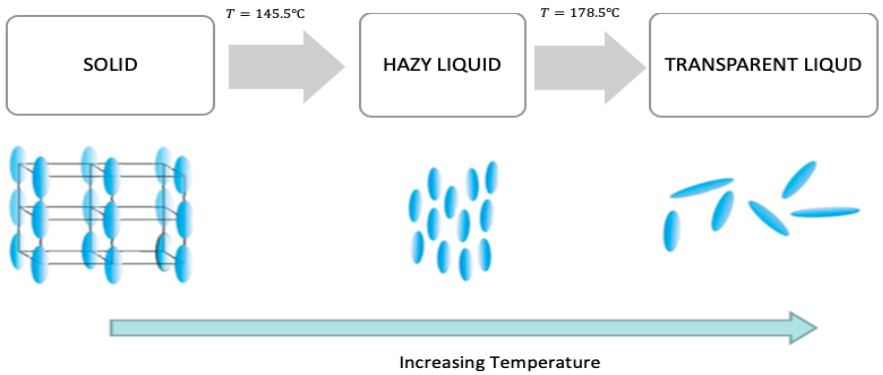

Figure 1: Schematic representation of the change of molecular order/packing of cholesteryl benzoate with temperature

Otto Lehmann, who specialised in crystallography and microscopy continued the studies that Reintizer started after receiving letters and samples from him. He started his investigations with cholesteryl benzoate and continued with related compounds. The systematic studies he performed confirmed the double melting observed by Reintizer. He also used a polarized microscope equipped with a hot stage enabling him to make investigations at high temperatures. He concluded that the observed cloudy melt maintained flow as well as some properties of solids and coined the term "*flüssiger Kristalle*" (liquid crystal, LC). As the initial studies belong to Reintizer, the discovery of the *liquid crystal phase* as a new state of matter is generally attributed to him [1].

Chronological Milestone:

- *1888 Friedrich Reintizer:* the strange melting behaviour of cholesterol, as having two melting points, was observed [2].
- *1890 Otto Lehmann:* the *liquid crystal phase* was identified as a novel peculiarity of matter [3].
- *1890 Gattermann and Ritschke:* p-azoxyanilosole, the first chemically synthesized material having a liquid crystal behaviour, was generated [4].
- *1903 Vorlander and co-workers:* first thermotropic smectic compound was synthesised [5].
- *1904 Merck-AG*: first commercial liquid crystals were introduced [1].
- *1907 Vorländer*: the polymorphism of liquid crystals was detected and a paper detailing the relation between chemical structure and liquid crystallinity was published [6].
- *1922 Friedel*: names *nematic, smectic and cholesteric* referring to the

subphases of liquid crystals were used. Defects in liquid crystals was observed and the orienting effect caused by electric fields was explained [7].

- *1930s Carl Oseen and co-workers*: the first theoretical study to produce a mathematical basis for understanding liquid crystal behaviour was conducted and the Order Parameter **S,** the averaged orientation of liquid crystals, was defined. Later a continuum theory was developed, by using the work of Oseen on the elastic properties of LC [8-10].
- *1930s-1950s:* as no application field was discovered scientists lost their interest in LC materials.
- *1958 Saupe and Maier*: a molecular theory of LCs not involving permanent dipoles was developed, which later gave rise to Maier-Saupe Theory [11].
- *1969***:** MBBA was discovered to display a nematic subphase at room temperature [12].
- *End of 1960s:* the first application fields of cholesteric LCs were suggested as temperature indicators, analytical metrology, cancer diagnostics and non-destructive testing of materials [13].
- *1968 George Heilmeier:* first liquid crystal displays, LCDs, were prototyped [14].
- *1969 Saupe:* pure smectic C subphase was discovered [15].
- *1970-71 Schadt and Helfrich:* the twisted nematic (TN) cell was invented [16].
- *1974 MacMillan and R. Meyer*: a mean-field theory for smectic mesophase was proposed [17].
- *1975 Patricia Cladis:* re-entrant nematic phase was observed [18].
- *1975 Bob Meyer:* ferroelectricity in liquid crystals was suggested [19].

- *1978 S. Chandrasekhar*: the existence of discotic liquid crystals was reported [20].
- 1980 *Yu* and *Saupe*: biaxiality in nematic mesophase was observed [21].
- *1980s-1990s:* LCDs took the place of the typical displays used in technological devices such as computers, televisions, calculators, watches, telephones, etc [21].
- *Present:* wide application fields in display and opto-electronic devices, side by side the health sciences, especially pharmaceutical usages in targeted drug delivery [13, 22-24].

1.2 Phases of Matter

Matter is a substance that occupies space and has inertia (resistivity against the changes in its velocity). In advanced material science, matter is comprised of different sorts of particles, each having both mass and size. More than 100 distinct atoms, which each constitute a unique chemical element, are known to exist. A molecule is formed by elements and to form a compound atoms and molecules may join [25].

In thermodynamics, a chemically and physically uniform or homogeneous quantity of matter is called *phase.* When phase changes from one form to another, a phase change/transition is said to have occurred. Energy is the capacity to cause change. Matter may exist in several states, also known as phases. Figure 2 gives the properties of the three well known states namely solid, liquid and gas [26].

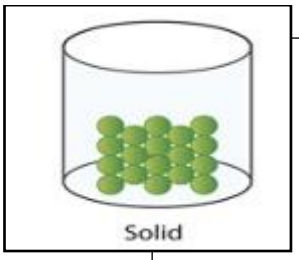

The particles of a solid are so strongly bonded that they have fixed positions, although the atoms have small vibrations as their electrons are in motion. Thus, solid particles have very low kinetic energy and definite shapes and volumes. As their particles are tightly packed together, they can not be compressed by increasing the pressure.

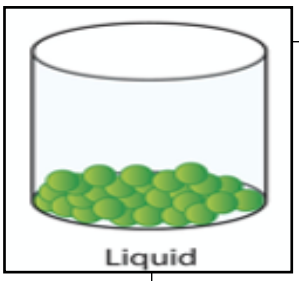

Compared to solids, the particles of a liquid are not regularly arranged. However, they still have enough bonding keeping them close to each other in a definite volume. As its particles have more freedom to move compared to solids they have more kinetic energy. Liquids are incompressible also. Because of their arrangements the particles of a liquid can flow, meaning liquids do not have a definite shape.

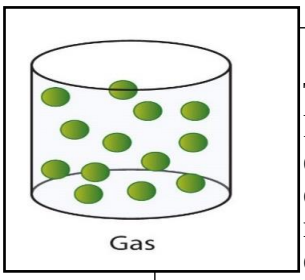

The space between gas particles is great as they have high kinetic energy. The gas particles are free to move and expand all arround, however if they are closed in a container they will fill the volume of the container. As the mentioned high energy of the gass particles are enough to overcome the bonding forces between them, gases have indefinite volume and shape.

Figure 2: Properties of the three well known phases and their schematic representations [25, 26]

The moment a solid is subjected to heat, its particles start to agitate faster due to the increase in their kinetic energy and thus move further apart. Upon heating, its temperature will start rising till it reaches the melting temperature. Solid and liquid phases coexist during phase transition and the temperature will stay constant until the whole sample is liquified [25, 26].

1.3 Liquid Crystal State

LC is a thermodynamic stable phase between a solid and a liquid, hence the term mesophase is used to define the subphases of LC, as represented in Figure 3. Compounds displaying LC properties are called mesogens [27].

A LC flows like a fluid but has the anisotropic properties of a crystal lacking the 3-dimensional lattice they possess. The molecules of a crystal have orientational order as well as 3-dimensional positional order, whereas the molecules do not have any long-range order in isotropic phases. In LCs, the particles neither have 3-dimensional positional order nor are they completely non-ordered [27, 28].

Different types of LC mesophases exist that are determined by various optical peculiarities such as textures. They show rare structural and physical characteristics [27-30].

There are 3 essential necessities a LC should meet [27-29]:

- LC mesophases must have first order phase transitions to isotropic liquid phase and solid phase, at high temperatures and low temperatures consecutively.
- In LCs the molecules must have 1 or 2-dimensional order only, as they are between a crystal (3-dimensional order) and an isotropic liquid (completely disordered).
- In a LC material some degree of fluidity must be present.

Figure 3: Structural order; crystalline phases, sub-phases of LC (mesophases), amorphous phases

1.3.1 Order in LCs

LC structures are described by using two main parameters as [27-30].

- Orientational order: Defines how the molecules tend to align along a specific direction in long-range.
- Positional order: Defines the range of translational symmetry regarding the position of a molecule or group of molecules.

Each parameter defines the amount of order the LC sample has. Generally, LCs display multi mesophases, so they are polymorphous.

1.3.1.1 Order Parameter (S)

The mean alignment direction of LC is called the vector director ($\hat{n}$) or simply director. The orientational order of a LC is defined by the order parameter (S), which is calculated by considering the deviation of each molecule from the director. The order parameter is defined as in Figure 4.

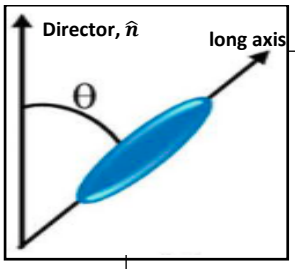

$$S = \left(\frac{1}{2}\right)\langle 3cos^2\theta - 1\rangle$$

θ is the angle between long axis of each molecule and the director, $\hat{n}$. The bracket is known as the average of all molecules in the sample.

Figure 4: Schematic representation and mathematical equation of the director ($\hat{n}$), long axis and the equation for calculating order parameter, S [27-29]

The average $\langle 3cos^2\theta - 1\rangle$ is zero in an isotropic liquid, and thus $S = 0$. The order parameter equals 1 for a perfect crystal, and every molecule is aligned parallel to the director. In LCs the typical values for order parameter are 0.85 < S < 0.95 for the smectic phase and 0.45 < S < 0.65 for the nematic phase. By using diffraction measurements, order parameters can be calculated.

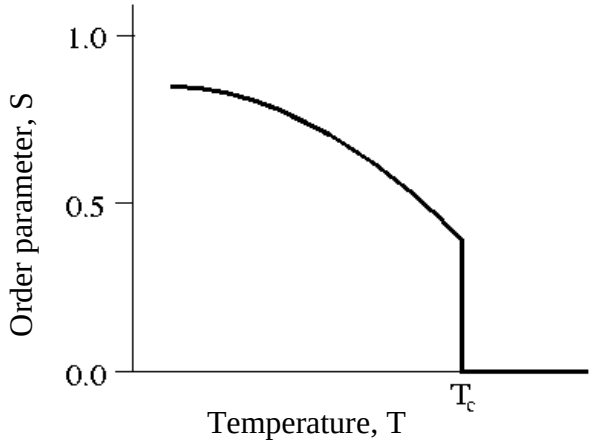

Figure 5: Plot of typical temperature, T, dependence of the order parameter, S. Tc represents the temperature at which LC to liquid phase transition occurs

The order parameter is temperature dependent. As can be seen in Figure 5, the increase in temperature decreases the order parameter and at a temperature denoted as T_c the order parameter immediately becomes zero, as the phase transition from mesophase to

isotropic liquid takes place. As the molecules of LC tend to lie along the director, they are anisotropic. This implies that the properties of LC rely on the direction in which the measurements are taken.

LCs have anisotropic nature like solids, and they can flow like liquids. This unique behaviour gives rise to a huge application field in science and technology [27-29].

1.4 Classification of Liquid Crystals

LCs are categorised into two major groups as thermotropic liquid crystals (TLC) and lyotropic liquid crystals (LLC), based on the effect inducing the phase transition [27-30].

1.4.1 Thermotropic Liquid Crystals, TLCs

LCs that undergo phase transitions only with thermal effects are categorised as TLCs and this type of phase transitions are called thermotropic phase transitions. Usually, pure compounds or mixtures of compounds fall into this category [31].

TLCs can be formed by different structural arrangements of their molecules as; be disc-shaped, rod-shaped, board-shaped, or bent-shaped. Schematic representations for those structural arrangements are given in Figure 6. Mesogens with level disk-shaped structural arrangements comprising of an adjoining aromatic ring centre, allowing two-dimensional ordering of columns, form discotic LCs. Mesogens with rod-shaped structural arrangements that have anisotropic geometry which permits for an arrangement along spatial course form calamitic LCs. Mesogens with board-shaped structural arrangements whose orientation reflects the symmetry of their constituent molecules form Sanidic LCs. Mesogens with bent-shaped structural order, which have polar order, although the molecules are not chiral form bent-core LCs [27, 30, 31].

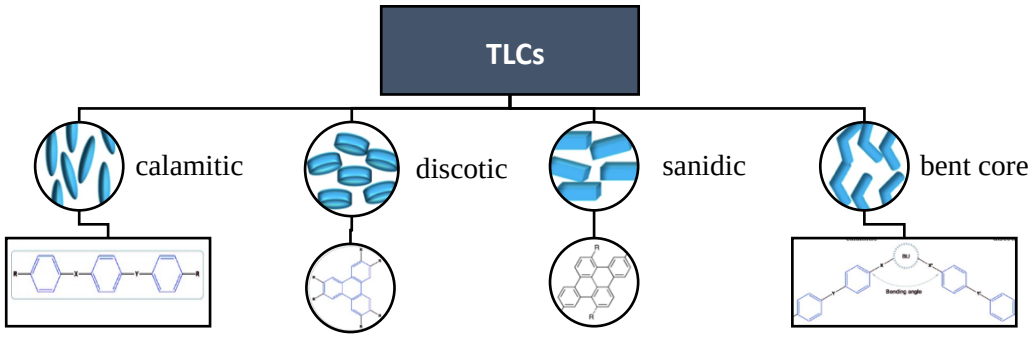

Figure 6: Classification of thermotropic LCs according to molecular arrangement with their schematic representations and example molecular structure [30, 31]

The thermotropic phase transitions can be reversible or irreversible [31]:

- Enantiotropic refers to the phase transitions that are reversible, in which the phase transition occurs both on heating and cooling.
- Monotropic refers to the phase transitions that are irreversible, in which the phase transition occurs only on heating or cooling, but not both.

1.4.2 Lyotropic Liquid Crystals, LLCs

LCs that undergo phase transitions not only with thermal effects but also with the changes in the concentration are called LLCs. LLCs display both thermotropic and lyotropic phase transitions.

LLCs are usually the mixtures of amphiphilic molecules consisting of polar and nonpolar parts with solutes such as water or oil. Anisotropic micelles are the basic units of these systems. Several distinct lyotropic mesophases can arise from different arrangements of these micelles, as represented in Figure 7. Amphiphiles can form several different types of micelles such as spheres, cylinders, and bilayers, under certain concentrations and temperature intervals, which then form lyotropic mesophase [28].

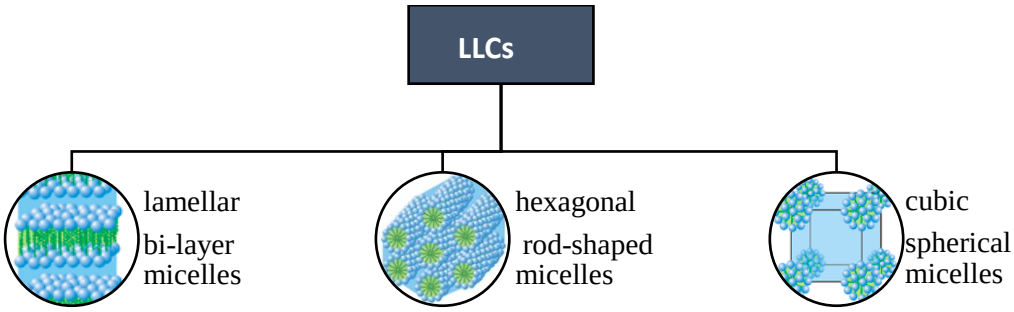

Figure 7: Different arrangement of micelles, lamellar-hexagonal-cubic, forming LLC mesophases [28]

Depending on the aim of the investigation, alcohol, organic, and inorganic salts can also be added to the sample.

Over limited ranges of composition and temperature, two mesophases will coexist [28]. Researchers have constructed significant number of phase diagrams for different binary lyotropic systems (BLSs) [32-39]. For each of the mesophases there is a direct phase transition from mesophase to isotropic liquid. The mesophases displayed by a BLS are formed again when more components are added to the system making it ternary lyotropic system (TLS) or a higher component system. With the addition of more components new mesophases that were not displayed by the binary system can also arise. The phase diagrams of those ternary or higher component systems are much more complex [28].

In nature, liquid lyotropic crystals occur widely, becoming widespread in living systems. Their mechanisms are complicated and not exactly clarified yet. In various everyday scenes, LLCs can be found in detergents, shampoos, and many other household items [40].

1.4.2.1 The Hydrophobic and Hydrophilic Effect - Amphiphilic Molecules

Water is the main solvent used in LLCs. The interactions between the amphiphilic molecules and water molecules are the primary effect responsible for the formation of the lyotropic mesophases. The interactions involved are electrostatic in nature, as water molecules have permanent dipole moments.

The term amphiphilic was coned per a Greek name amphi, meaning duo or dual, and phile, meaning like or love. It is used to describe molecules consisting of a hydrocarbon chain that is insoluble in water alongside a polar group that is soluble in water. These parts are referred as hydrophilic and hydrophobic, represented in Figure 8 as an example [28].

- Hydrophilic: have a strong affinity for water, i.e., it is attracted to water, and can dissolve in water.
- Hydrophobic: not attracted to water, it resists mixing with water, the opposite of hydrophilic.

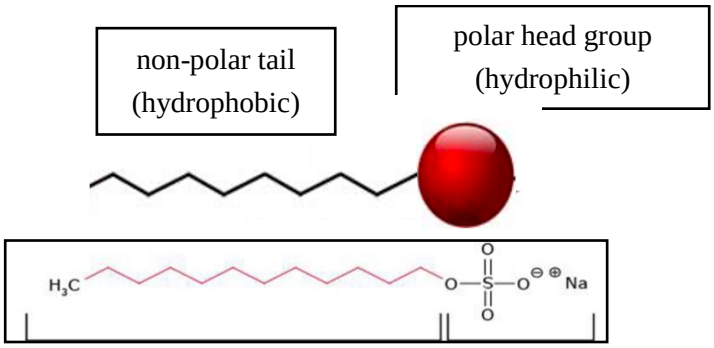

Figure 8: Representation of an amphiphilic molecular structure, sodium dodecyl sulphate

There are various types of amphiphilic molecules that are chemically synthesized: anionic amphiphiles (fatty acid soaps, e.g., potassium laurate), detergents (e.g., sodium decylsulfate); cationic amphiphiles (e.g., hexadecyl trimethylammonium bromide);

non-ionic amphiphiles (e.g., pentaethyleneglycol dodecyl ether); and zwitterionic amphiphiles (e.g., hexadecyl trimethylammonium bromide). Lyotropic mesophase are formed when anelydes (wetting agent) are added to amphiphilic molecules.

There are molecules having multiple polar groups that form lyotropic mesophases also, as represented in Figure 9 [27, 28].

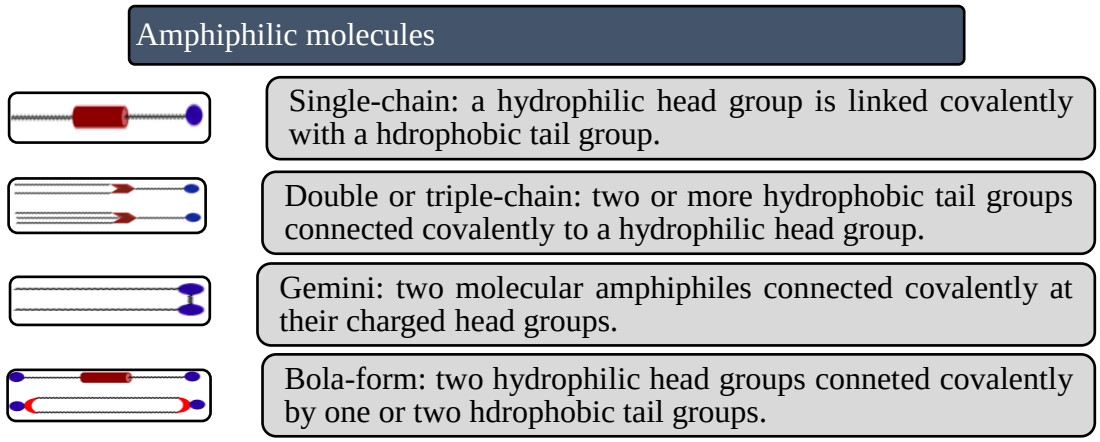

Figure 9: Types of amphiphilic molecules

1.4.2.2 Critical Micelle Concentration

When amphiphilic molecules meet with water, majority of the molecules will disperse, while some will move to the surface to prevent the contact of water with their hydrocarbon tails. Aggregates (or micelles) begin to form, to prevent the contact between the hydrophobic tails and the aqueous environment, at a concentration called critical micelle concentration (CMC) [27, 28], as represented in Figure 10.

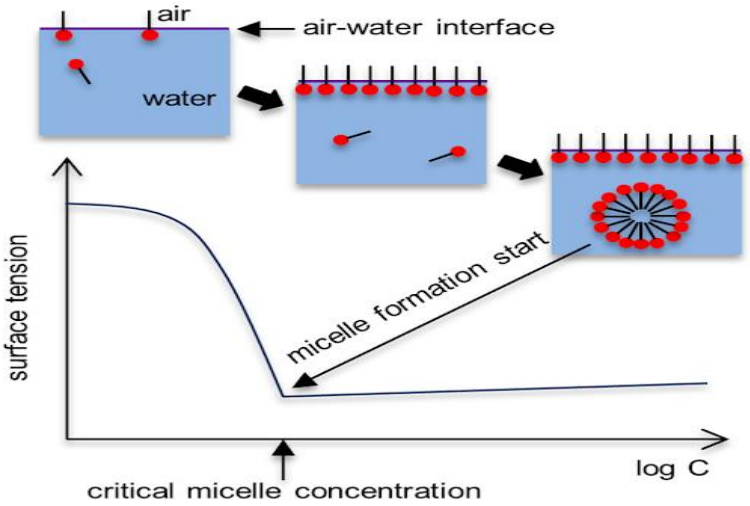

Figure 10: Critical Micelle Concentration

Considering that the nature of these molecules is fluid like we can determine the form of micelles by looking at how the amphiphiles pack together. The equation used for this determination is given as.

$$critical\ packaging\ parameter, cpp: \qquad \gamma = \frac{V}{a_0 l_c}$$

Where V is the volume of hydrocarbons, a_0 is the optimum area for the head group and l_c is the critical chain-length in Figure 11 [27, 28].

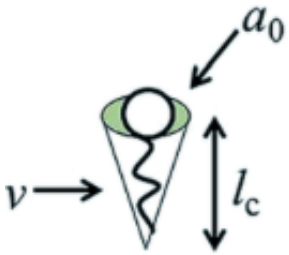

Figure 11: The schematic representation of an amphiphile with the parameters needed to define Cpp

1.5 LLC Mesophases

1.5.1 Isotropic Micellar L_1 Phase

As aforementioned, when amphiphiles are added into a solvent, which is mainly water, the aggregated amphiphiles will start to form micelles/reverse micelles, because of their nature, after the critical micelle concentration. Before the concentration of the amphiphile is enough to form other structures. LLC mesophase, the micelles will disperse in the solvent. Such a solution is isotropic and called a micellar solution, hence Isotropic Micellar L_1 phase [28, 30].

1.5.2 Hexagonal E Mesophase

E mesophase is the first ever reported lyotropic mesophase by McBain, in a soap + water system. In the hexagonal or middle phase, the layers are packed into cylinders, and those cylinders having indefinite length are arranged parallel to each other in a hexagonal array, as shown in Figure 12. This mesophase is uniaxial, with an optical axis parallel to the long axis of the micelles, and forms at concentrations higher than those of micellar L_1 phase at certain temperature intervals [28, 30].

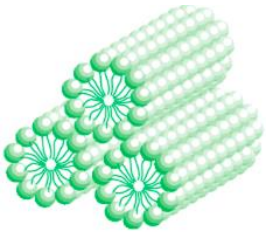

Figure 12: Schematic representation of the structure of hexagonal mesophase

1.5.3 Nematic Mesophase

Nematic mesophases were first introduced in quaternary systems by Lawson and Flautt, and Reeves simultaneously, consisting of amphiphile + inorganic salt + alcohol + water in 1967. Today binary, ternary, and quaternary systems displaying nematic

mesophases are known [28, 30, 32, 33, 35, 40]. Anionic, cationic or zwitterionic amphiphiles lead the formation of those mesophases. There are three forms of nematic mesophases identified: the nematic calamitic, N_C, mesophase that is produced by rod like micelles, the nematic discotic, N_D, mesophase produced by discs likes micelles and optically biaxial, N_{Bx}, mesophase as represented in Figure 13.

The structure of N_{Bx}, discovered in 1980s, is not completely understood yet. The cholesteric mesophase is often referred to as the chiral nematic mesophase is not considered as a type of nematic mesophase but the chiral form [28, 30].

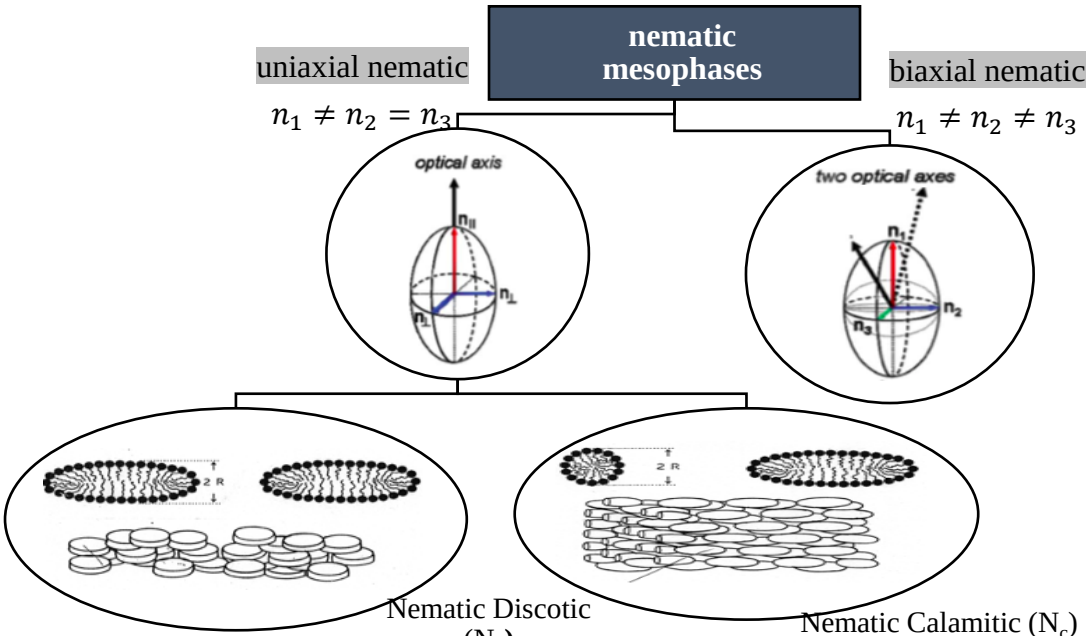

Figure 13: Schematic representation of the structures and optical axes of nematic mesophases

1.5.4 Cholesteric Mesophase (Chiral Nematic)

Cholesteric mesophase is characterised as having long-range orientational order however it does not have long-range positional order when mass centres of molecules are considered. The cholesteric mesophase is close to the nematic mesophase, however

it differs from the nematic mesophase as its director's direction changes constantly. When a nematic mesophase aligned along the y-axis is twisted along the x-axis, the structure of cholesteric mesophase is obtained.

The structure is charecterised by its pitch, as shown in Figure 14. The length of this pitch is in the wavelenght of visible light, several hundred nanometres. The spiral structure derives the typical colours displayed by the cholesterics, through Bragg reflection.

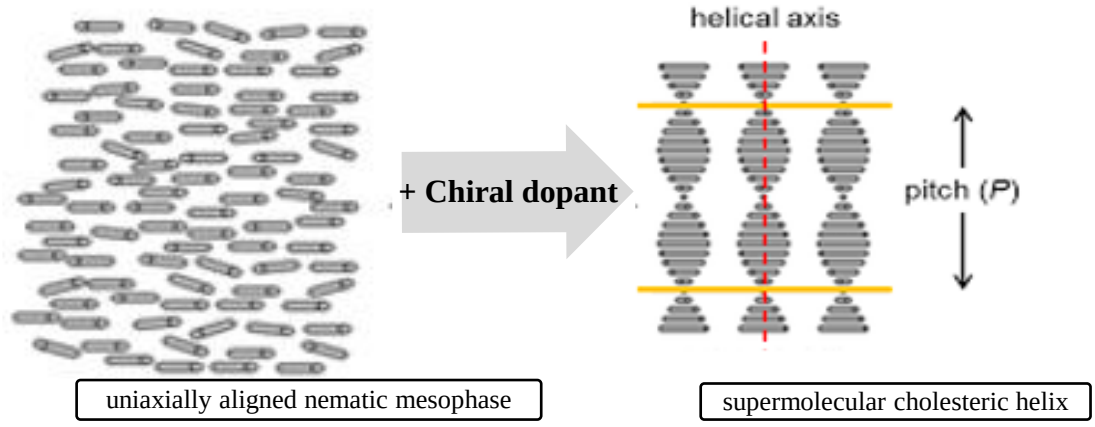

Figure 14: Schematic representation of the structures of uniaxial nematic and cholesteric mesophases

Chiral materials with large twisting power have reported to display Blue Phases, in a very narrow temperature range between a chiral nematic phase and an isotropic liquid phase [28, 30].

1.5.5 Lamellar D Mesophase

The most common lamellar mesophase is the “soap boilers’ neat soap”, first studied by McBain. It forms at extremely high amphiphile concentrations, 60-90%. The arrangement in lamellar mesophase is such that the polar heads sandwich water molecules, keeping the disordered hydrocarbon tails in a non-polar environment as

represented in Figure 15. Lamellar mesophase can be in balance with all the other mesophases in amphiphile + water systems via two–phase or three–phase regions.

In binary systems of amphiphile + water the lamellar mesophase forms before the solid crystalline phase at low water concentrations (high amphiphile concentrations) and/or after the hexagonal E mesophase at higher concentrations of water (lower concentrations of amphiphile).

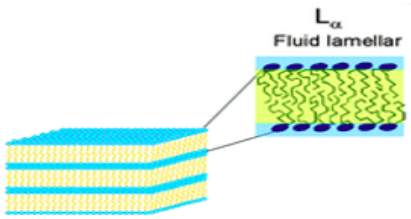

Figure 15: Schematic representation of the structure of lamellar mesophase

Lamellar mesophase, with 1-10 poise viscosity values, is in a mucous form through its existence region and the sample is half transparent and optically anisotropic [28, 30].

1.6 Applications of Liquid Crystals

The initial usage of LCs were the thermometers that were based on the temperature dependence of the cholesteric LC pitch. Whereas flat panel display technologies are the predominant application for LCs (LCDs). According to their anisotropic behaviour and their sensitivity to electrical fields, liquid crystals are present in the display devices of all technologic equipment. Liquid crystals have broad variety of applications because of their electro – optical, magneto – optical, electro – chromic, and thermo – chromic peculiarities. Biological membranes, DNA, and RNA are few examples of important biological structures. LCs are invaluable in manufacturing and medical applications [29, 41, 42].

Applications are still being discovered for this unique kind of material and continue to have useful solutions to several issues. LCs are part of our daily life.

1.7 Aims and Objectives.

The aim of this research is to determine the effect of salt on the phase states and physical parameters of a BLS. To reach this purpose the followings steps will be followed:

- ✓ The phase diagram of TTAB + water BLS will be constructed.
- ✓ The phase diagram will be reconstructed using 95 $wt\%$ water + 5 $wt\%$ salt as the solvent, instead of water itself.
- ✓ The RI – temperature and electroconductivity – temperature dependences will be defined for both systems.
- ✓ The obtained phase diagrams will be compared to understand the effect of salt on the thermotropic, mesomorphic and polymorphic behaviour of the BLS.
- ✓ The physical property – temperature dependences will be compared for the samples with same amphiphile concentrations to understand the effect of salt on the physical parameters of BLS.

Chapter 2

EXPERIMENTAL METHODOLOGY

2.1 Preparation of Lyotropic Liquid Crystal Samples

LLC systems are sensitive. For this reason, to obtain reliable and accurate results, a clean laboratory environment and tools are necessary. In addition, the components need to be weighted in high sensitivity when preparing the samples. For this purpose, we used a precision scale with a draft shield, having a sensitivity of $10^{-4}g$ (Ohaus AX224).

Tetradecyl trimethyl ammonium bromide (TTAB - Sigma, cat. No.: T4762) as the amphiphile, sodium bromide (NaBr - BioXtra, cat. No: S4547) as the inorganic salt, and ultra-pure water as solvent were used in the preparation of samples. TTAB and NaBr had high purity degree, $\geq 99\%$, and were used as bought. All compositions were prepared as wt-wt%.

In order to prepare the ternary sample, a homogeneous mixture of NaBr and water was obtained. Then, TTAB and the homogeneous mixture were mixed in desired amounts in glass vials. The glass vials were hermitically sealed and all samples were held in a thermoset at constant temperature, $310\,K$, till they become homogenous. The homogeneities of the samples were tested through texture homogeneity analysis before the samples were used for investigations.

Scale	Glass vial and cup	Thermostat	Schematic representation of sandwich-cell type plane capillaries. 1- referance glass surfaces 2- spacer

Figure 16: Equipment used for sample preparation

Figure 16 represents the equipment used during sample preparation. Sandwich-cell type plane capillaries were prepared for the investigations with Polarized Optical Microscope. The thickness of the liquid crystalline layer was fixed as 70μm.

2.2 Polarizing Optical Microscopy (POM)

LC systems display textures which reflect the arrangement of micelles forming them, and this arrangement changes due to the changes in concentration and/or temperature of the composition. LC mesophases exhibit a definite number of specific and non-specific textures with various morphological and optical characteristics. The unique textures make it possible to classify the mesophases [30]. The POM method is used to observe and analyse the textures displayed by LC mesophases. This technique is of great significance as it offers the ability to evaluate not only the mesophases, but also the regions of phase transition [41].

There is a polychromatic light source, polarizer, and analyser in a standard POM. The target is set while the eyepiece is moved to the necessary magnification. The polarizers and analysers are crossed, so there is no visible light. When a liquid crystal is added, the polarization plane is rotated by liquid crystal and a texture is seen in the microscope.

Optical Mapping is the main and most widely used method to identify the mesophases by texture analysis. In this method, the textures examined using POM are matched with the specific textures of the mesophases in the literature to identify the mesophases [30].

Recording, retrieval and saving features are available. The texture seen via the eyepiece can be pictured or video recorded by using a high-resolution pixel camera, mounted to the microscope. A special software can be used to measure the dimensions/areas of the formations seen in the textures if needed. Hot and cold stages can also be used to investigate the changes in the texture dynamics by temperature. Optical filters, λ-plates, special lenses etc. can be added to the system whenever needed.

2.2.1 Experimental Setup

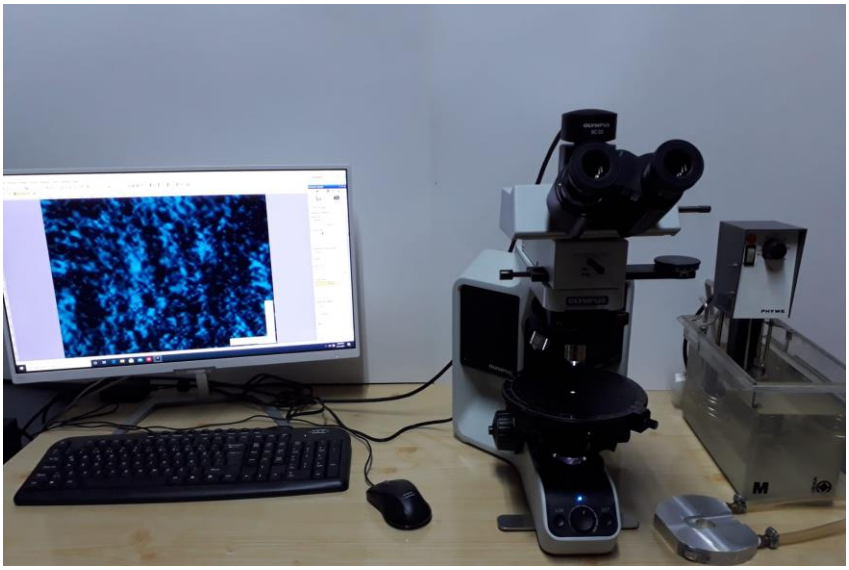

Figure 17: Experimental setup used for POM investigations

The setup, represented in Figure 17, consists of polarized microscope (Olympus BX53M), microphotographic system (Olympus SC35), a special software (Olympus

cellSens Entry 2), and a custom-made heater thermostat system with temperature control.

2.3 Refractive Index Measurements

Refractometry is known to be the most appropriate method used to determine the refractive indices (RI) of transparent and semi-transparent samples. RI is generally dependent on the temperature of the material and this method allows us to measure the changes in refractive index with the changes in temperature [42]. Once the temperature dependences of RI values are obtained for the system, it is also possible to obtain the concentration dependences of the RI values at constant temperatures. LCs are optically anisotropic and birefringent (or bi-refractive), their refractive indices depend on the direction of polarization and the direction of propagation of light.

When light enters to a birefringent medium it separates into two rays, namely ordinary and extraordinary. The electric vector of the ordinary ray is perpendicular to the optical axis whereas it is parallel for an extraordinary ray. As being birefringent materials, LCs have two RI values corresponding to those two rays, ordinary RI ($n_o = n_\perp$) and extraordinary RI ($n_e = n_\parallel$). The difference $\Delta n = n_e - n_o$ gives the value of the birefringence and generally $n_e > n_o$ the birefringence value is positive, $\Delta n > 0$, for most of the LCs [30].

Abbé refractometer is the oldest and most frequently used tool for measuring the refractive index of an optical material [43]. Abbé refractometers use the critical angle principle. Light enters the sample through illuminating prism and reflects from the bottom of the measuring prism at a critical angle. A rotary knob on the Abbé refractometer is used to adjust the mirror so that the position of the boundary between

light and dark regions intersects with the crosshairs of the telescope. Once the adjustment mentioned is achieved, the refractive index and the temperature of the sample can be read from the vernier scale and digital display respectively. The picture is inverted by the telescope, so the black region appears towards the bottom, even though it should be at the upper portion of the field of vision. The matted surface of the illuminating prism provides light entrance to the sample in all possible angles. A schematic representation of Abbé refractometer's optical system is shown in Figure 18.

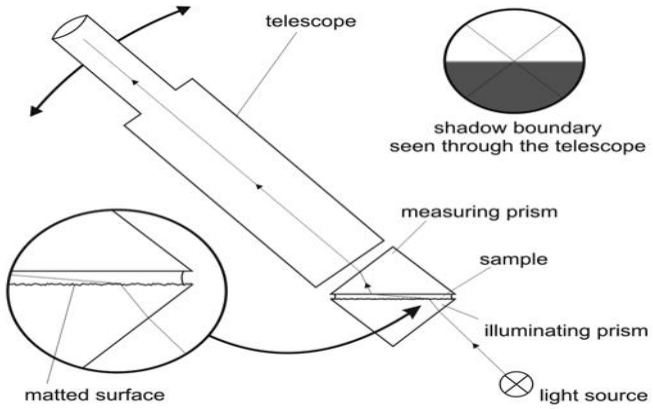

Figure 18: Schematic diagram of Abbé refractometer (light entering the illuminating prism producing dark and bright regions in the field of view)

Abbé refractometers can measure the RI values both for solids and liquids, with a fourth decimal place accuracy of roughly one to two units [43].

2.3.1 Experimental Setup

Figure 19: Experimental setup used to determine RI – temperature dependences

The setup, represented in Figure 19, includes a Deluxe Illuminated Abbé Refractometer (Krüss AR4) and a thermostatic water circulation system (Phywe).

2.4 Electroconductivity Measurements

Electrical conductivity, σ, is a material property which determines how well electricity will be conducted by a given sample [38]. Electrical conductivity is inversely related to resistivity via the equation $\sigma = \frac{1}{\rho}$. Conductivity measures the total amount of ions in a solution, but since it is unable to differentiate between electrolytes or ions, it is not specific. Conductivity measurements are classified as either contacting or inductive. The inductive method is used when the sample has high conductivity, suspended solids or is corrosive. The contacting approach was used in this study.

Most contacting conductivity probes have sensors made of stainless steel or titanium electrodes. The electrodes that are in contact with the sample produce an electric field

when subjected to an alternating voltage, forcing the ions in the sample to move, thus, generate an ionic current. The conductance of the sample is calculated by the analyser using current and voltage.

A conductivity probe with four electrodes is used in this investigation. Four-electrode sensors eliminate the charge transfer effects at the metal-liquid interface as the voltage measurement circuit consumes minimal current, providing a significantly larger measuring range [45].

2.4.1 Experimental Setup.

Figure 20: Experimental setup used to determine electroconductivity – temperature dependences

The experimental setup, represented in Figure 20, consists of Thermo Scientific Orion Versa Star VSTAR90, VSTAR-CBD Conductivity Module, Electrode Stand, Orion™ DuraProbe™ 4-Electrode Conductivity Cells, and thermostatic water circulation system (Phywe).

Chapter 3

RESULTS AND DISCUSSION

3.1 TTAB + Water BLS

3.1.1 Phase States

To define the phase states, compositions prepared as sandwich cells were analysed under a polarized optical microscope and the mesophases existing were detected and identified by observing the typical textures representing them. All the compositions were also subjected to heating during the investigations and the mesophase – isotropic liquid thermotropic phase transitions were observed and recorded.

The investigations showed that the system did not display any color i.e., it was all black between crossed polarizers below $37.2\ wt\%$ TTAB concentration. That reflects the isotropic behavior of those samples meaning a micellar solution, L_1 phase, is present at concentrations ranging from $CMC - 37.2\ wt\%$ TTAB.

The first texture observed after the L_1 phase region was complicated, not specific for any mesophase, consisting of formations belonging to the texture of nematic-calamitic N_C mesophase side by side black regions, showing the coexistence of L_1 phase and N_C mesophase. It was defined that L_1 phase and N_C mesophase coexist in a narrow range of $37.2 - 37.4\ wt\%$ TTAB, representing L_1 – N_C lyotropic phase transition region.

When samples with TTAB concentrations higher than $37.4\ wt\%$ were investigated, they were defined to be anisotropic, mesophases form beyond this concentration. Two concentration intervals that samples display specific textures, representing distinct mesophases, were identified. Between those mesophase intervals, complicated textures, including texture characteristics from more than one mesophase, were observed. Those regions represent the coexistence of mesophases, which are lyotropic phase transition intervals.

In the concentration interval $37.4 - 38.8\ wt\%$ TTAB, a texture that is represented in Figure 21a, well known from the literature [47-51] and specific for N_C mesophase was observed. This interval represents the region where N_C mesophase exists.

The texture observed after the N_C mesophase region was again complicated, consisting of formations belonging to the texture of N_C mesophase as well as E mesophase showing their coexistence. N_C and E mesophases were observed to coexist in the concentration interval of 38.8 - $39.9\ wt\%$ TTAB, representing N_C – E lyotropic phase transition region.

The existence of E mesophase was defined for the samples starting from $39.9\ wt\%$ TTAB concentration. The texture observed given in Figure 21b, is a specific texture of E mesophase, that is well known from the literature [47, 49-51]. It should be noted that we were not able to obtain a homogenous mixture above $47.0\ wt\%$ TTAB.

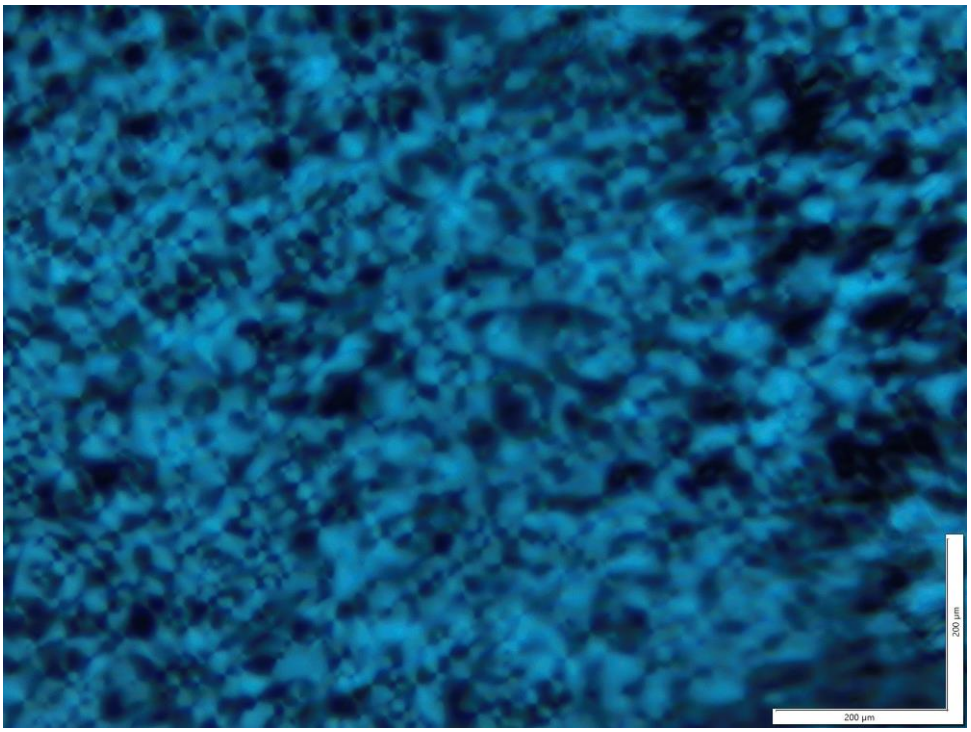

(a)

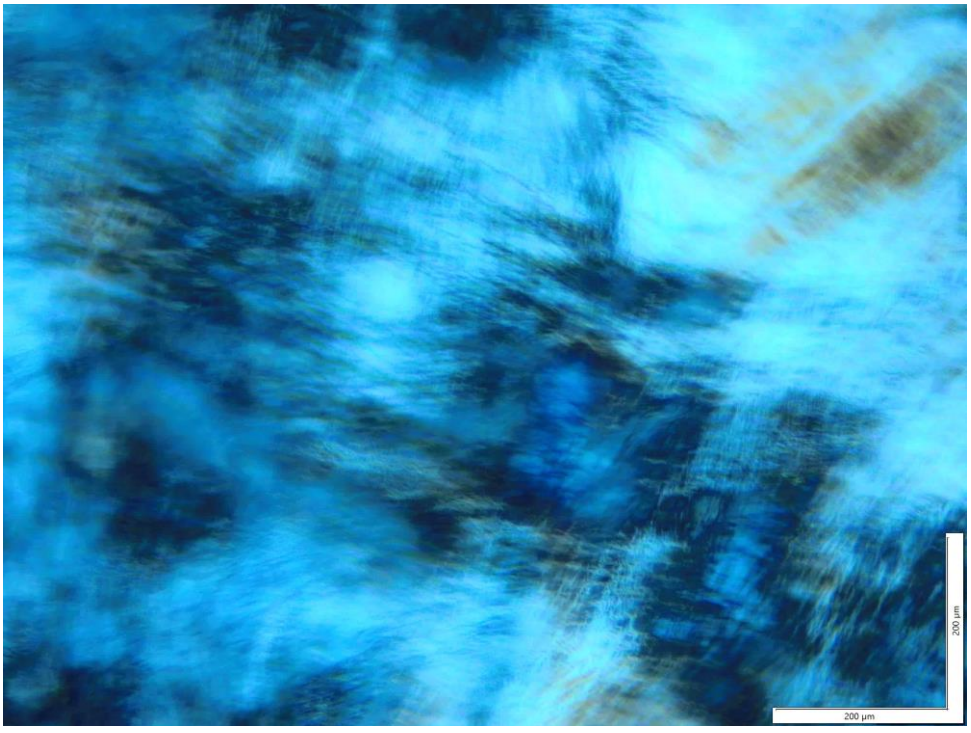

(b)

Figure 21: The textures (a) N_C, (b) E mesophases displayed by TTAB + water BLS with 200µm scale

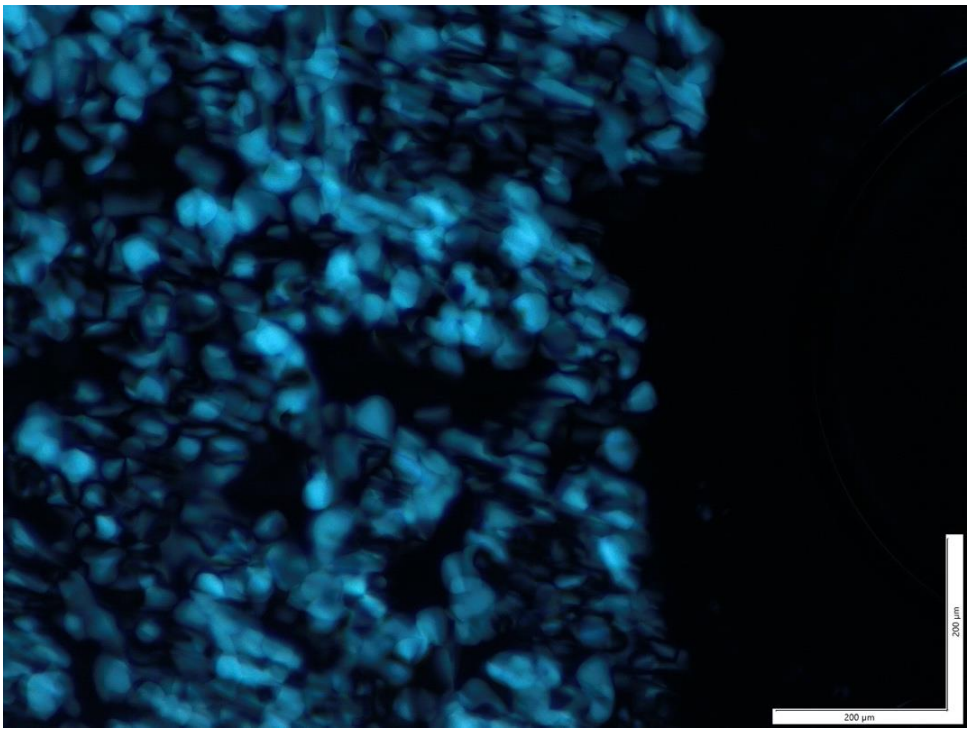

(a)

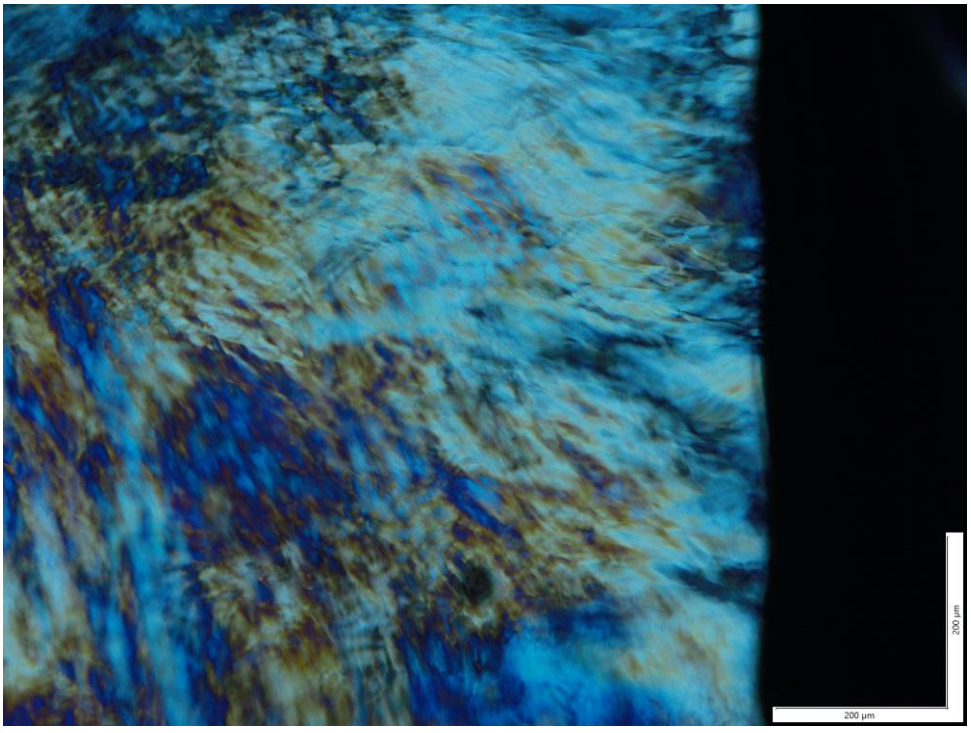

(b)

Figure 22: Mesophases melting into isotropic liquid, both with $200\mu m$ scale (a) N_C mesophase – L_1 phase thermotropic phase transition (b) E mesophase – L_1 phase thermotropic phase transition

As aforementioned, the thermotropic phase transitions of the system were also investigated and the phase transition temperatures were defined. Figure 22 represents the textures of N_C and E mesophases melting into isotropic liquid at thermotropic phase transition temperatures respectively.

As examples, the sample of N_C mesophase with $38\,wt\%$ TTAB concentration melts into L_1 phase at $315K$ and the sample of E mesophase with $41\,wt\%$ TTAB concentration melts into L_1 phase at $329K$. The obtained transition temperatures can be seen from the temperature axis of the constructed phase diagram which is given in Figure 23.

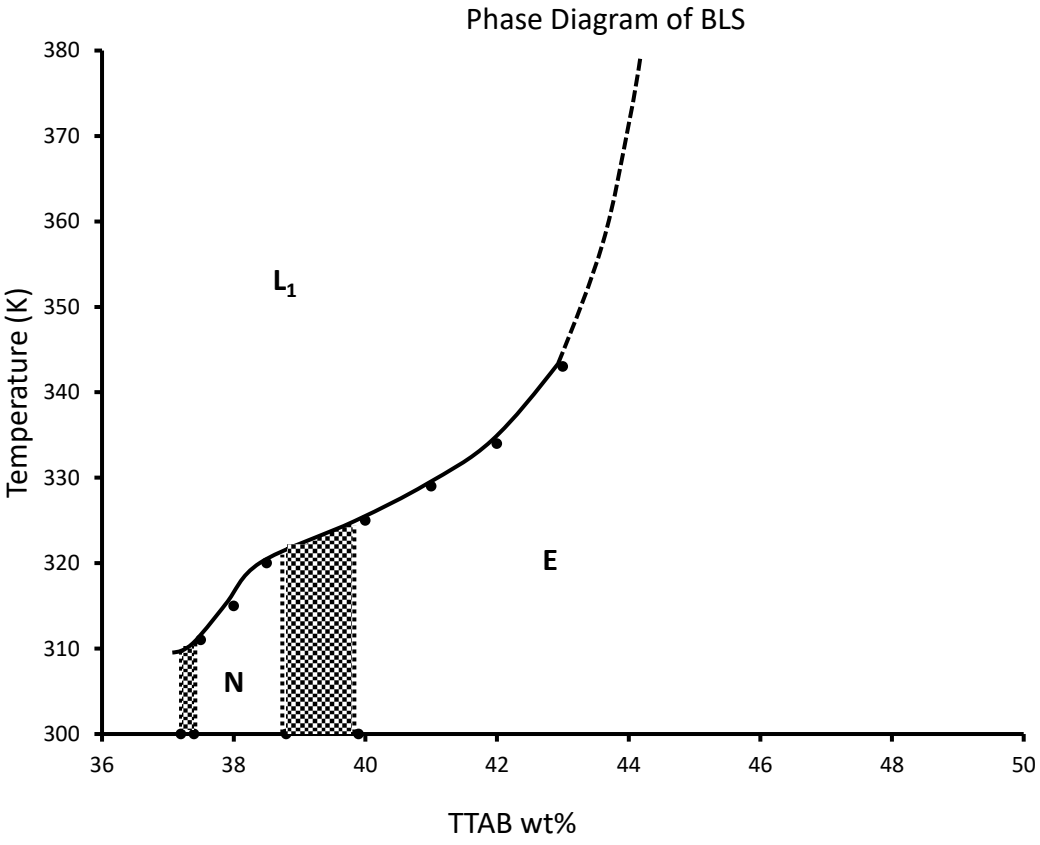

Figure 23: The phase diagram of TTAB + water BLS

3.1.2 Physical Parameters

The changes in refractive index (RI) and electroconductivity values of TTAB + water system was investigated over large temperature and concentration intervals. The refractive index – temperature, $n = f(T)$, and electroconductivity – temperature, $\sigma = f(T)$, dependences of all mesophases defined for the mentioned system were investigated and represented.

The defined refractive index – temperature dependences are given in Figures 24, 25 and 26 for L_1 phase, N_C mesophase and E mesophase regions respectively.

The analysis of the given dependences shows that the refractive indexes decrease linearly with the increase in temperature for all the samples investigated. As is known, the density of an LLC usually decreases with increasing temperature. Thus, the speed of light increases with increase in temperature which is reflected as decreases in RI values. As so, this result was expected and is in correlation with the literature [34, 48, 49, 52].

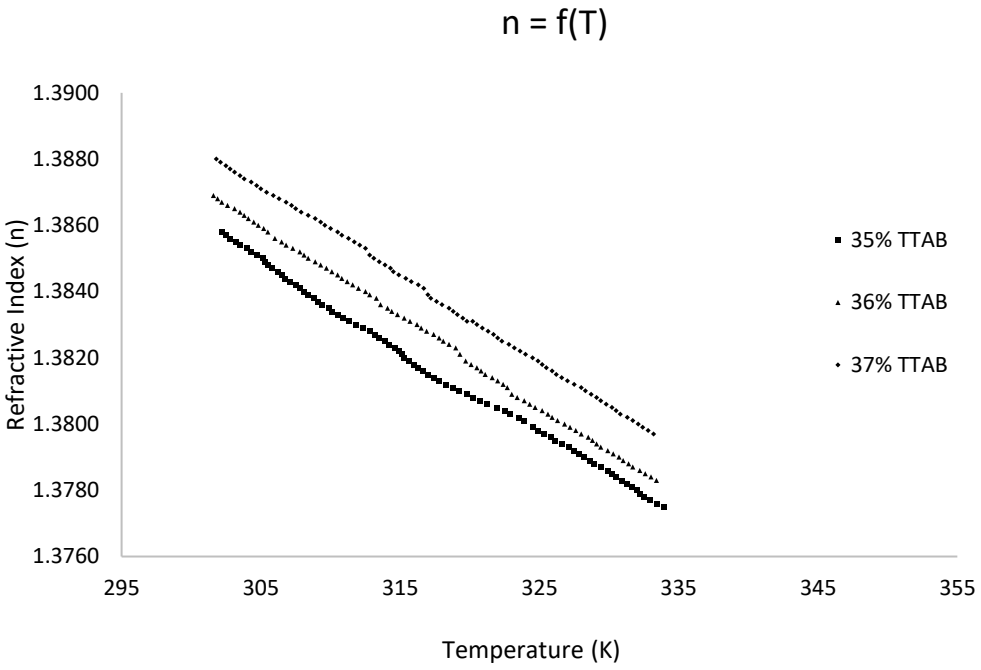

Figure 24: $n = f(T)$ dependences for L_1 phase. (Samples with 35 $wt\%$ TTAB + 65 $wt\%$ water, 36 $wt\%$ TTAB + 64 $wt\%$ water and 37 $wt\%$ TTAB + 63 $wt\%$ water compositions)

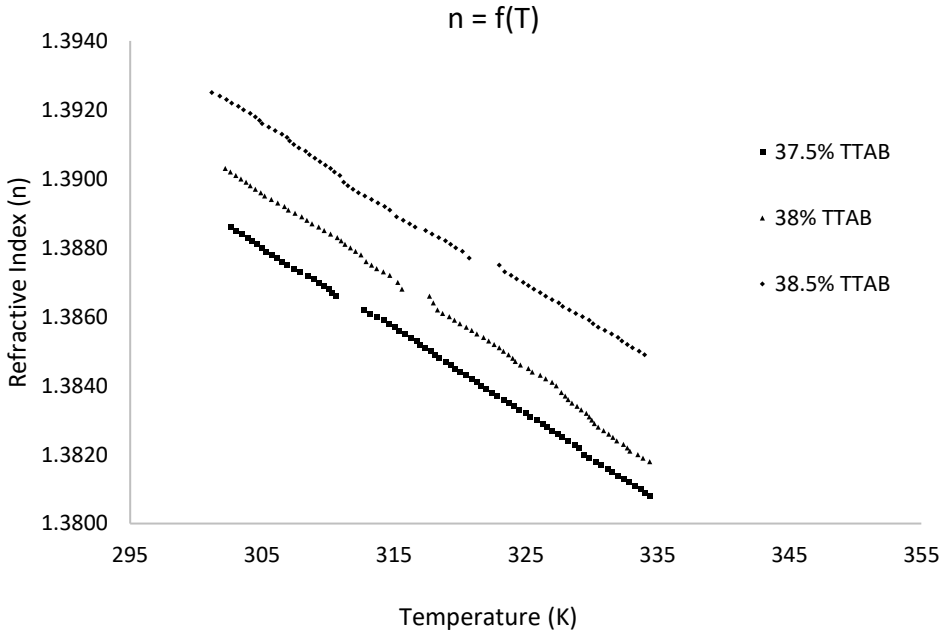

Figure 25: $n = f(T)$ dependences for N_C mesophase. (Samples with 37.5 $wt\%$ TTAB + 62.5 $wt\%$ water, 38 $wt\%$ TTAB + 62 $wt\%$ water and 38.5 $wt\%$ TTAB + 61.5 $wt\%$ water compositions)

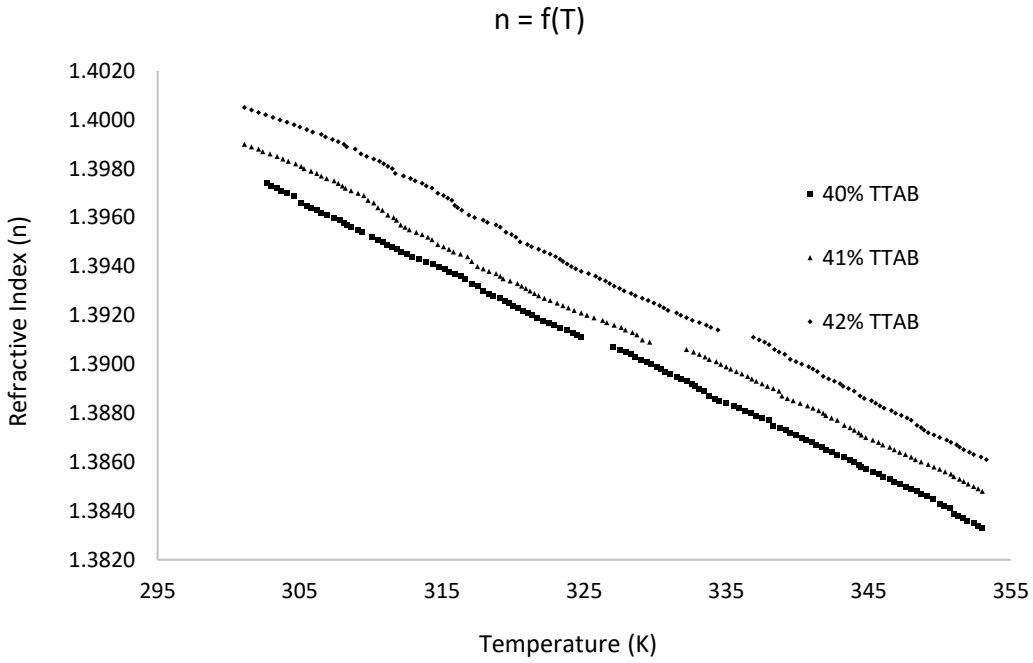

Figure 26: $n = f(T)$ dependences for E mesophase. (Samples with 41 $wt\%$ TTAB + 59 $wt\%$ water, 42 $wt\%$ TTAB + 58 $wt\%$ water and 43 $wt\%$ TTAB + 57 $wt\%$ water compositions)

Figures 27, 28 and 29 represent the temperature dependences of conductivity values. The analysis of the given dependences shows that the conductivity values increase exponentially with the increase in temperature. As the ions will have more kinetic energy, thus will be more mobile when their temperature is increased, this result was also expected [45, 53].

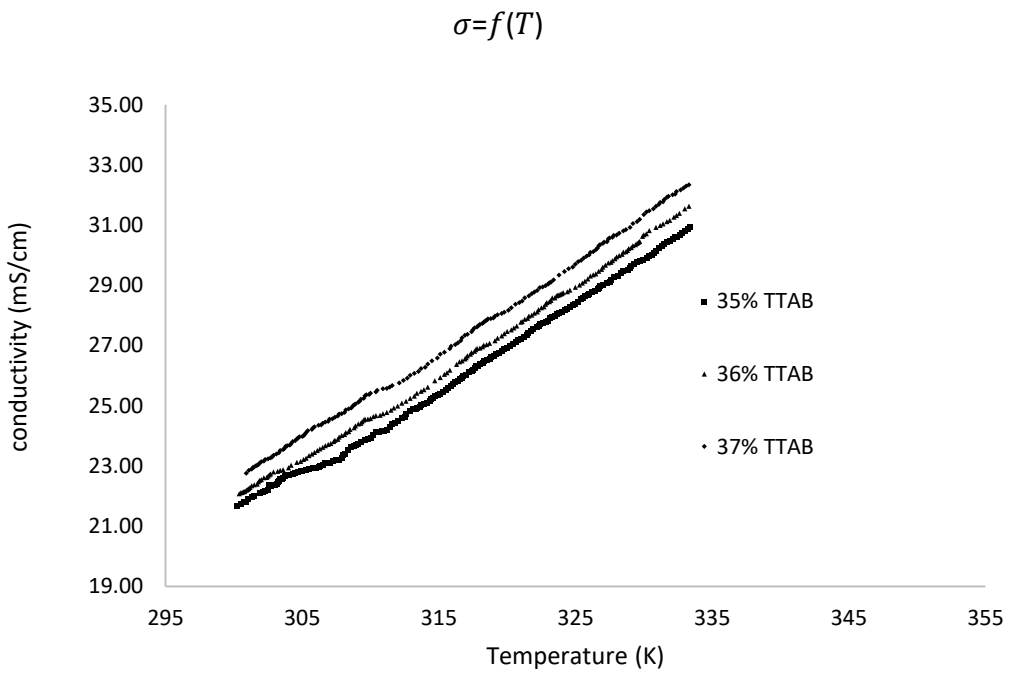

Figure 27: $\sigma = f(T)$ dependences for L_1 phase. (Samples with 35 $wt\%$ TTAB + 65 $wt\%$ water, 36 $wt\%$ TTAB + 64 $wt\%$ water and 37 $wt\%$ TTAB + 63 $wt\%$ water compositions)

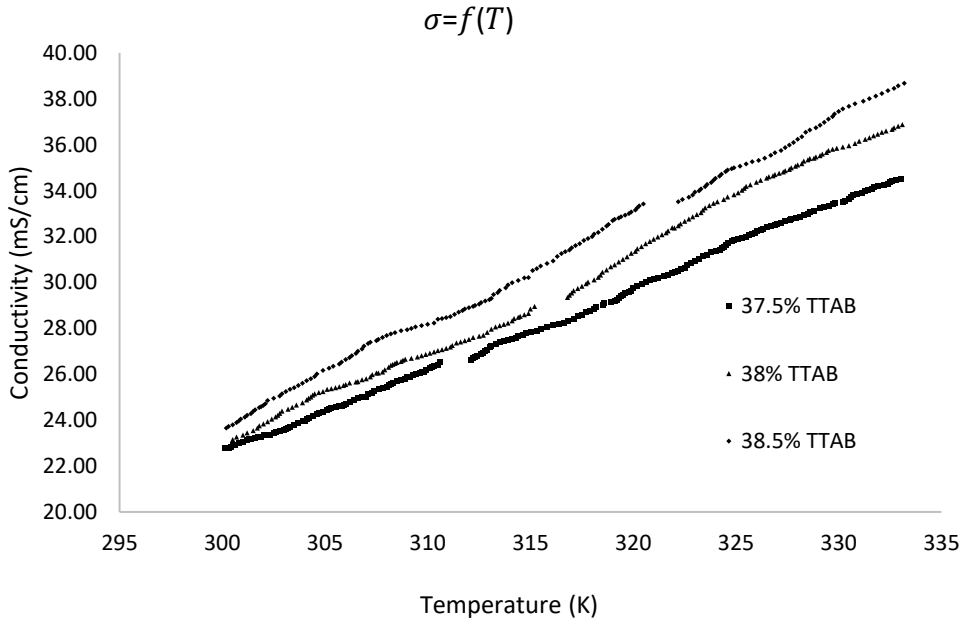

Figure 28: $\sigma = f(T)$ dependences for N_C mesophase. (Samples with 37.5 $wt\%$ TTAB + 62.5 $wt\%$ water, 38 $wt\%$ TTAB + 62 $wt\%$ water and 38.5 $wt\%$ TTAB + 61.5 $wt\%$ water compositions)

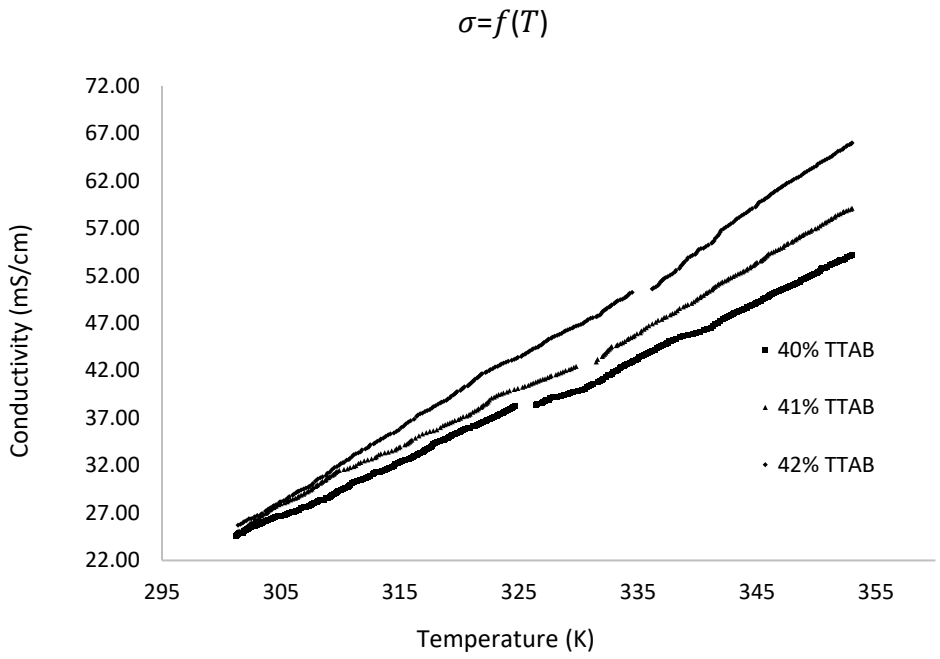

Figure 29: $\sigma = f(T)$ dependences for E mesophase. (Samples with 41 $wt\%$ TTAB + 59 $wt\%$ water, 42 $wt\%$ TTAB + 58 $wt\%$ water and 43 $wt\%$ TTAB + 57 $wt\%$ Water compositions)

The analysis of the $n = f(T)$ and $\sigma = f(T)$ dependences shows that the change is unremitting, without any anomalies, for all the compositions for L_1 phase. However, those dependences show some anomalies at certain temperature intervals for all compositions belonging to mesophases. Since physical parameters of a sample results from its structure, we can conclude that the structure of the sample does not change with temperature in the L_1 phase interval however, it does in the mesophase intervals. If we take the structural change as a phase transition, we simply understand that there is no thermotropic phase transition for L_1 phase however, the mesophases show thermotropic phase transitions. Comparing the temperatures that those anomalies appear, in the $n = f(T)$ and $\sigma = f(T)$ dependences, it can be seen that they are almost same for samples with equal compositions, and they match with the thermotropic phase transition temperatures obtained in POM investigations, as given in Table 1.

Table 1: Thermotropic phase transition temperatures obtained by different methods; POM, $n = f(T)$ dependences and $\rho = f(T)$ dependences.

TTAB concentration	**phase/mesophase**	**phase transition temperature obtained from POM**	**anomaly temperature on $n = f(T)$ dependence**	**anomaly temperature on $\rho = f(T)$ dependence**	**Corresponding thermotropic phase transition**
35 $wt\%$	L_1	-	-	-	-
36 $wt\%$	L_1	-	-	-	-
37 $wt\%$	L_1	-	-	-	-
37.5 $wt\%$	N_C	311.2 K	310.8 K	311 K	$N_C - L_1$
38 $wt\%$	N_C	315.6 K	315.2 K	315 K	$N_C - L_1$
38.5 $wt\%$	N_C	320.7 K	320.5 K	320 K	$N_C - L_1$
41 $wt\%$	E	329.6 K	329.8 K	329 K	$E - L_1$
42 $wt\%$	E	334.4 K	334.5 K	334 K	$E - L_1$
43 $wt\%$	E	343.1 K	342.0 K	343 K	$E - L_1$

With increase in temperature, the conductivity increases for LLCs [34, 42,45]. When the observed graphs are analyzed, it comes out that the change in conductivity by temperature is exponential, rather than the relation in refractive index case which was determined to be linear.

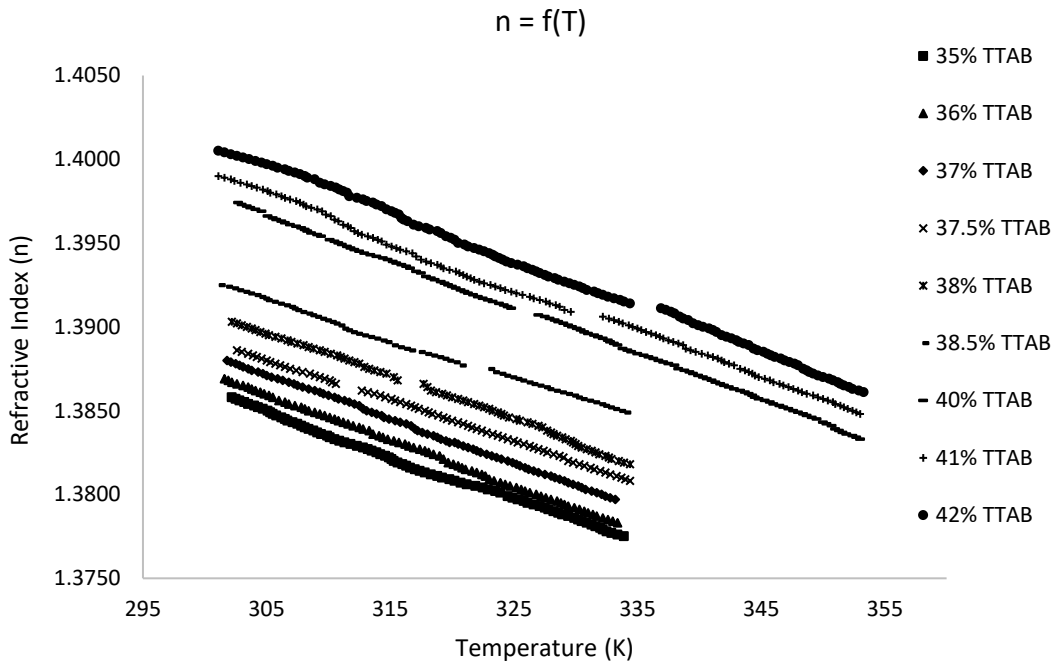

Figure 30: $n = f(T)$ dependences for TTAB + water BLS

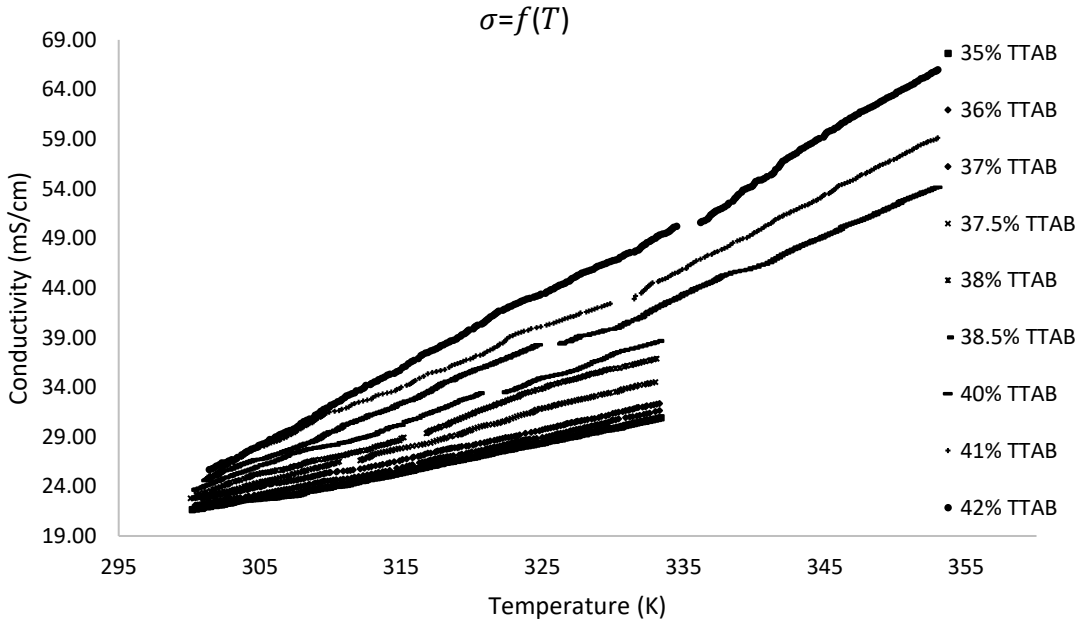

Figure 31: $\sigma = f(T)$ dependences for TTAB + water BLS

When the graphs are examined, we can see that the conductivity values are increasing also with the increase in amphiphile concentration.

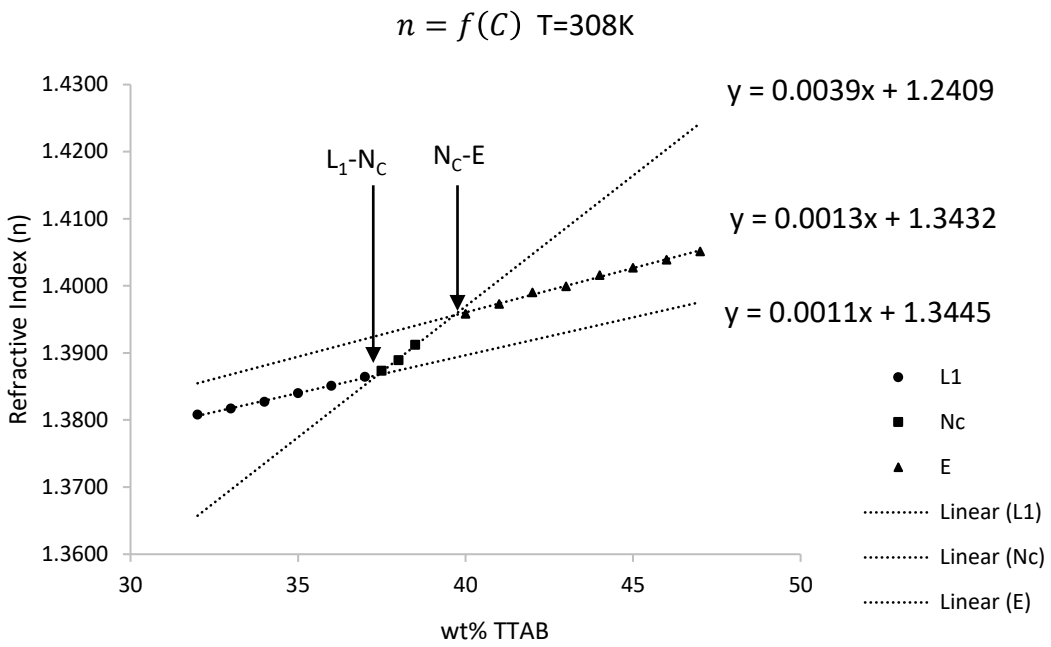

Figure 32: $n = f(C)_T$ dependence for TTAB + Water BLS at 308K

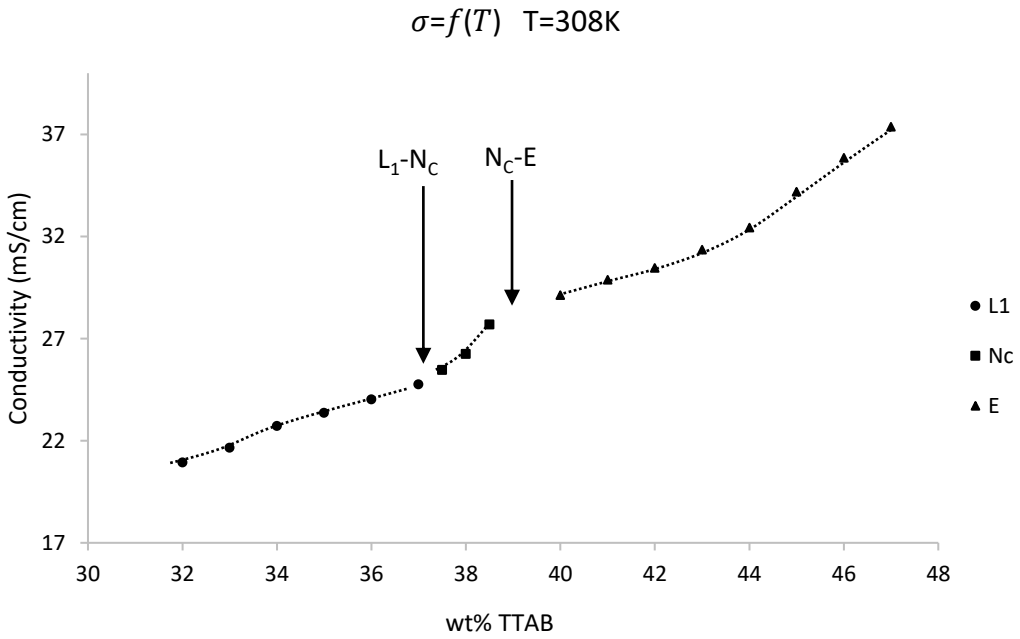

Figure 33: $\sigma = f(C)_T$ dependences for TTAB + Water BLS at 308K

Figure 30 and Figure 31 represents the $n = f(T)$ dependences and $\sigma = f(T)$ dependences for TTAB + water BLS respectively. When analyzed, both RI values and electroconductivity values increase with increasing amphiphile concentration for all compositions/mesophases of the system.

The concentration dependences of RI and electroconductivity at constant temperature are represented in Figure 32 and Figure 33 respectively. Following the same understanding we used to define thermotropic phase transitions from temperature dependence graphs, now we expect to define the lyotropic phase transitions from concentration dependence graphs. Those dependences are comprised of three different parts each corresponding to a different phase/mesophase. When compared with POM observations, we see that these dependences meet our expectations to define the lyotropic phase transition regions.

The defined phase states, thermotropic and lyotropic phase transitions, refractive index and conductivity ranges and their behaviour is in correlation with study [34].

3.2 TTAB + Water + Salt TLS

3.2.1 Phase States

As the focus of this study is to understand the effect of salt on a BLS, instead of constructing a ternary phase diagram we preferred to change our solvent from ultrapure water to 95 wt% ultrapure water + 5 wt% NaBr and construct a pseudo-binary phase diagram. The same manner and procedure used to investigate the phase states of BLS was repeated and the phase states, phase intervals, thermotropic and lyotropic phase transitions were defined for pseudo-BLS (pBLS).

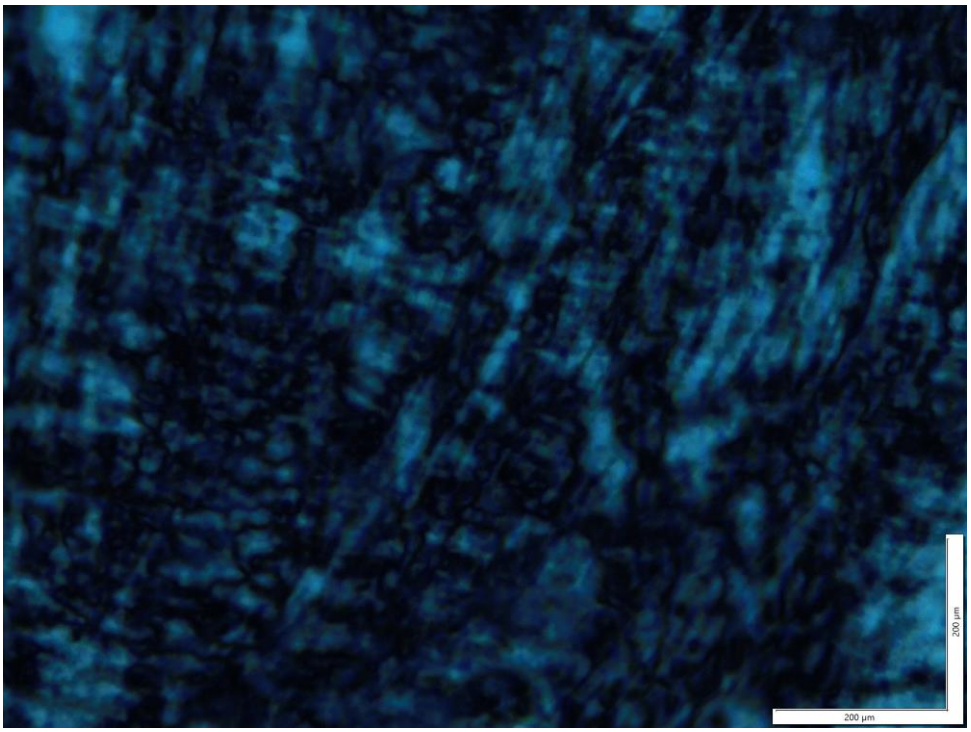

(a)

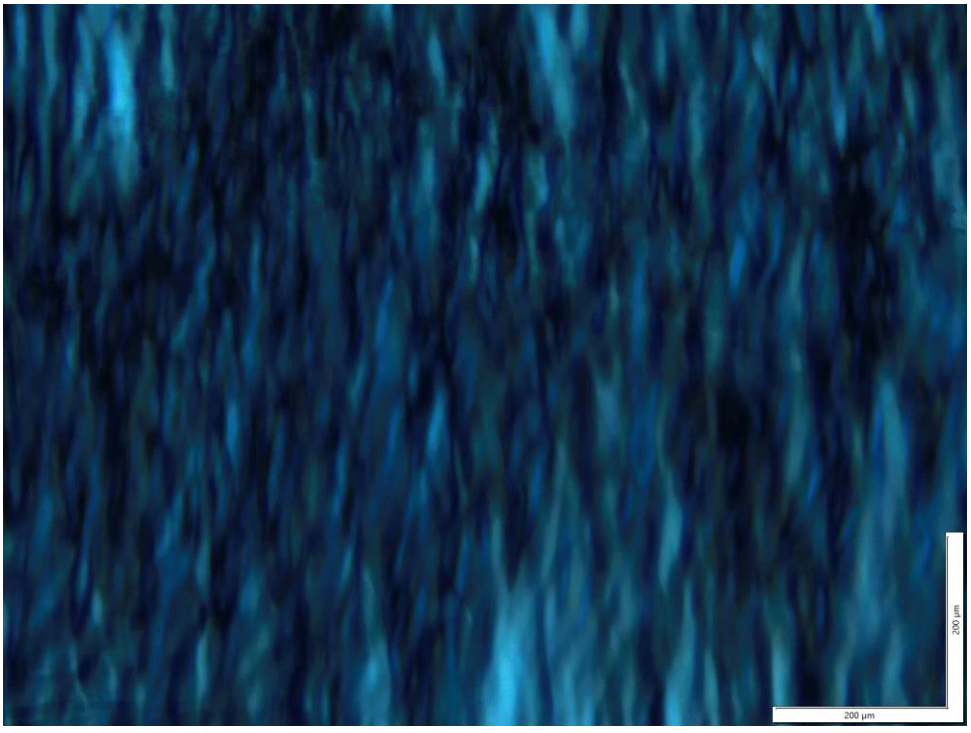

(b)

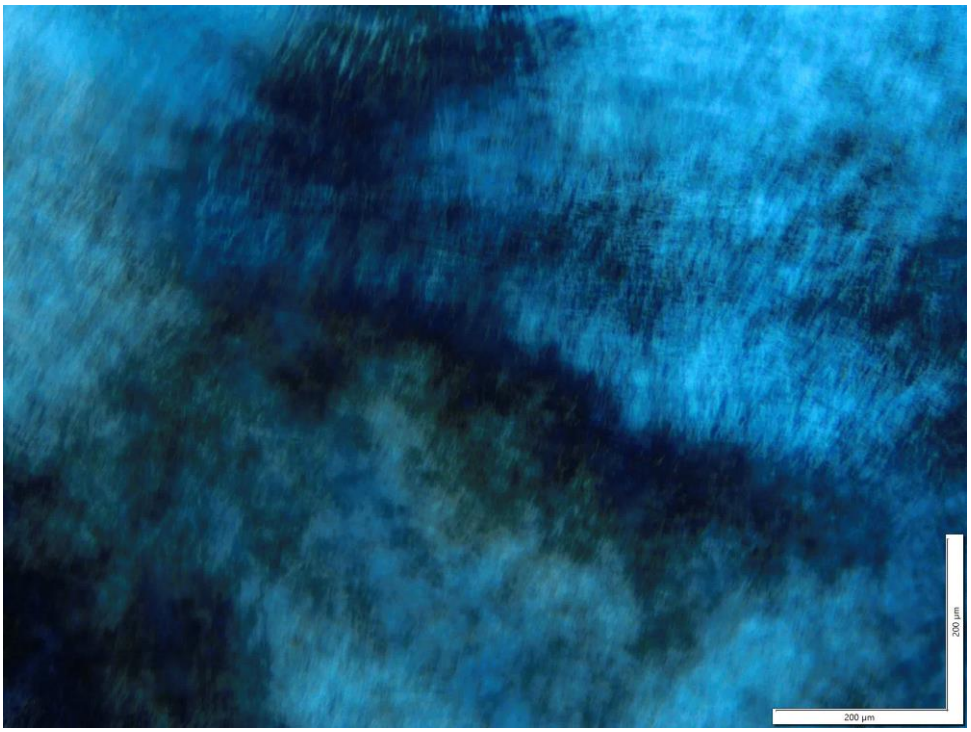

(c)

Figure 34: The textures observed for (a) N_C (b) N_D (c) E mesophases for TTAB + water + NaBr TLS

The investigations show the existence of four phases/mesophases in this system. Figure 34 represents the typical textures observed for the system, which all are well known from the literature [47-51]. The system is defined to display L_1 phase in the interval CMC$-37.8\,wt\%$ TTAB, N_C mesophase in the interval $38.4\,wt - \%\,41.2\,wt\%$ TTAB, N_D mesophase in the interval $42.5\,wt\% - 43.5\,wt\%$ TTAB and E mesophase after $43.8\,wt\%$ TTAB.

The lyotropic phase transitions were defined to be $37.8 - 38.4\,wt\%$ for L_1 – N_C, $41.2 - 42.5\,wt\%$ for N_C - N_D and $43.5 - 43.8\,wt\%$ for N_D – E. The thermotropic phase transitions of the system at certain concentrations was also investigated, again with the same procedure as in BLS. As example, N_C mesophase with $38.5\,wt\%$ TTAB concentration melts into L_1 phase at $321K$.

The obtained transition temperature can be seen from the temperature axis of the constructed phase diagram, represented in Figure 35. The E – L_1 phase transition temperatures could not be obtained as those temperatures are above $373K$, which is not possible to reach with a water circulation system.

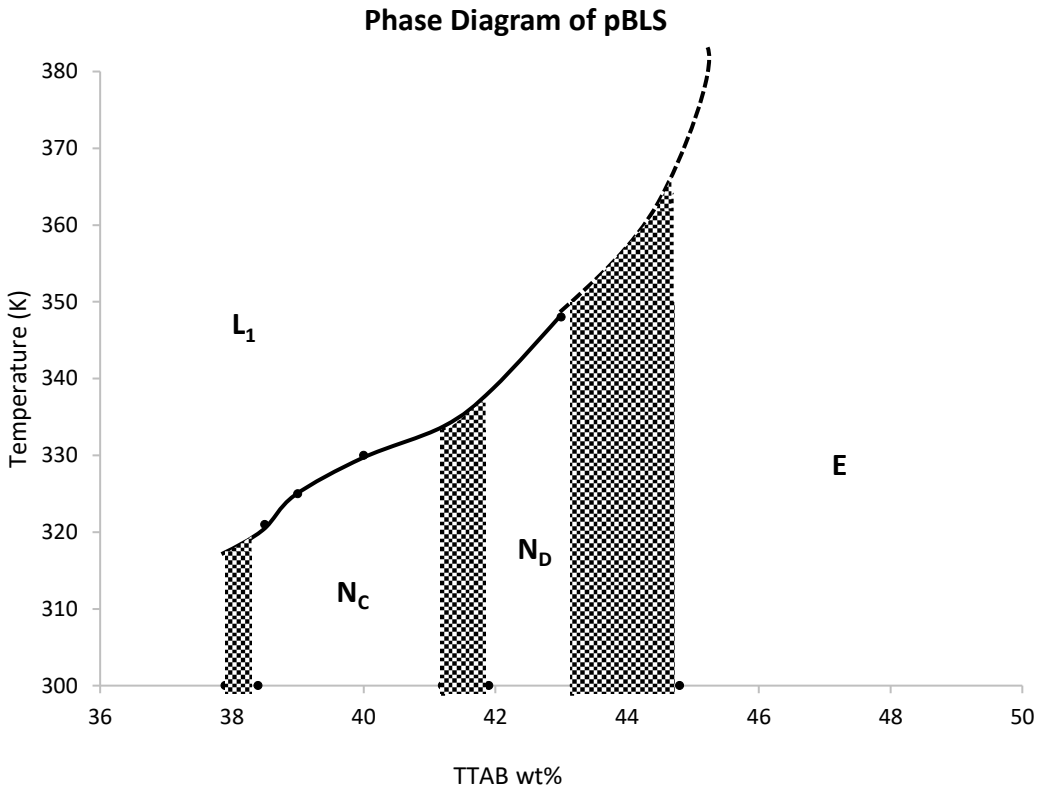

Figure 35: Phase Diagram of TTAB + salty water (95 $wt\%$ ultrapure water + 5 $wt\%$ NaBr) pBLS

3.2.2 Physical Parameters

The same manner and methodology used to investigate the physical parameters of the BLS are repeated for the ternary compositions corresponding the same amphiphile concentrations.

The defined refractive index – temperature dependences for L_1 phase, N_C mesophase and E mesophase are given in the Figures 36, 37 and 38 respectively. Figures 39, 40

and 41 represents the defined electroconductivity – temperature dependences of L_1 phase, N_C mesophase and E mesophase regions respectively.

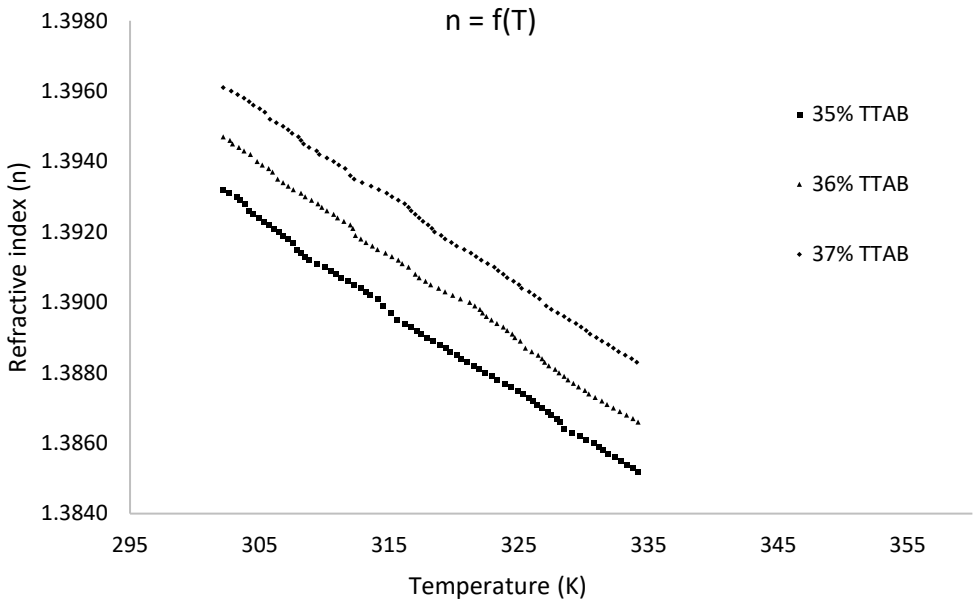

Figure 36: $n = f(T)$ dependences for L_1 phase. (Samples with 35 $wt\%$ TTAB + 65 $wt\%$ salty water, 36 $wt\%$ TTAB + 64 $wt\%$ salty water and 37 $wt\%$ TTAB + 63 $wt\%$ salty water compositions)

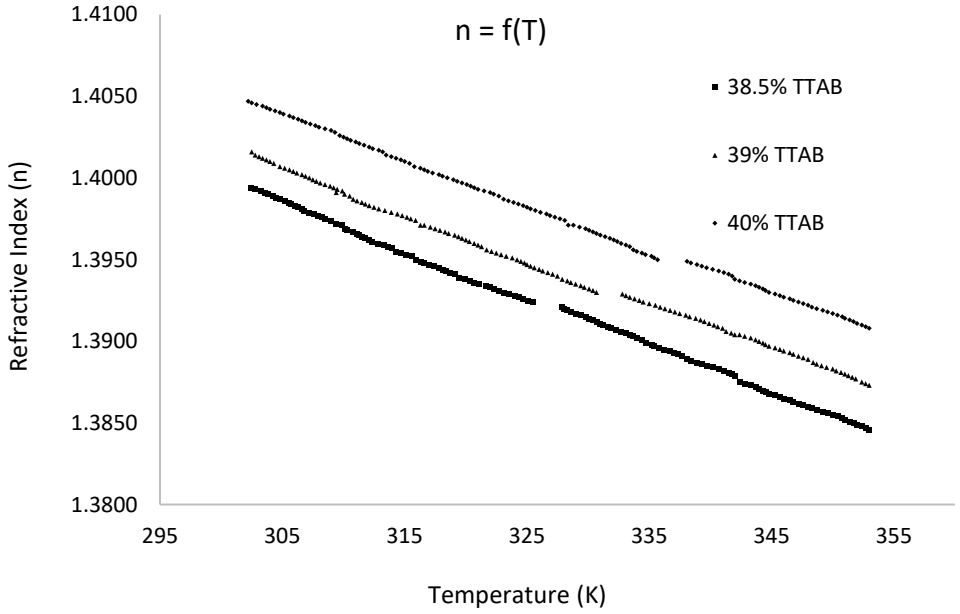

Figure 37: $n = f(T)$ dependences for N_C mesophase. (Samples with 38.5 $wt\%$ TTAB + 61.5 $wt\%$ salty water, 39 $wt\%$ TTAB + 61 $wt\%$ salty water and 40 $wt\%$ TTAB + 60 $wt\%$ salty water compositions)

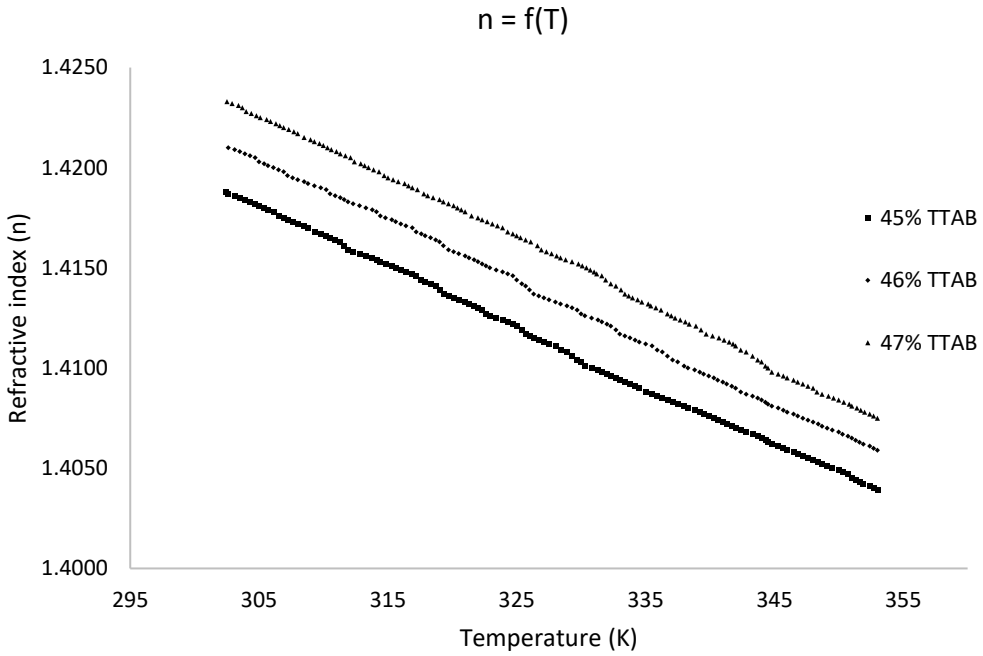

Figure 38: $n = f(T)$ dependences for E mesophase. (Samples with 45 $wt\%$ TTAB + 55 $wt\%$ salty water, 46 $wt\%$ TTAB + 54 $wt\%$ salty water and 47 $wt\%$ TTAB + 53 $wt\%$ salty water compositions)

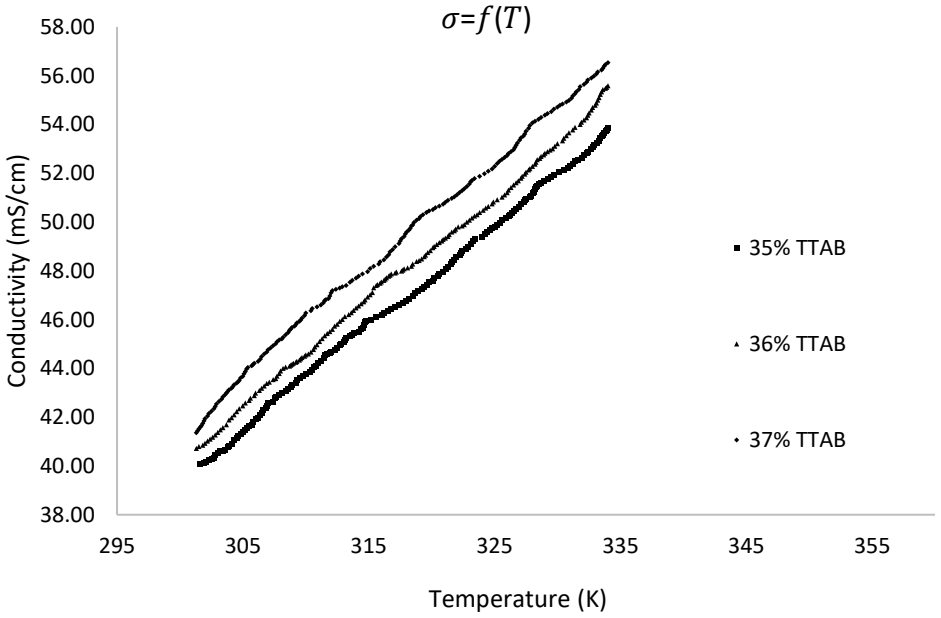

Figure 39: $\sigma = f(T)$ dependences for L_1 phase. (Samples with 35 $wt\%$ TTAB + 65 $wt\%$ salty water, 36 $wt\%$ TTAB + 64 $wt\%$ salty water and 37 $wt\%$ TTAB + 63 $wt\%$ salty water compositions)

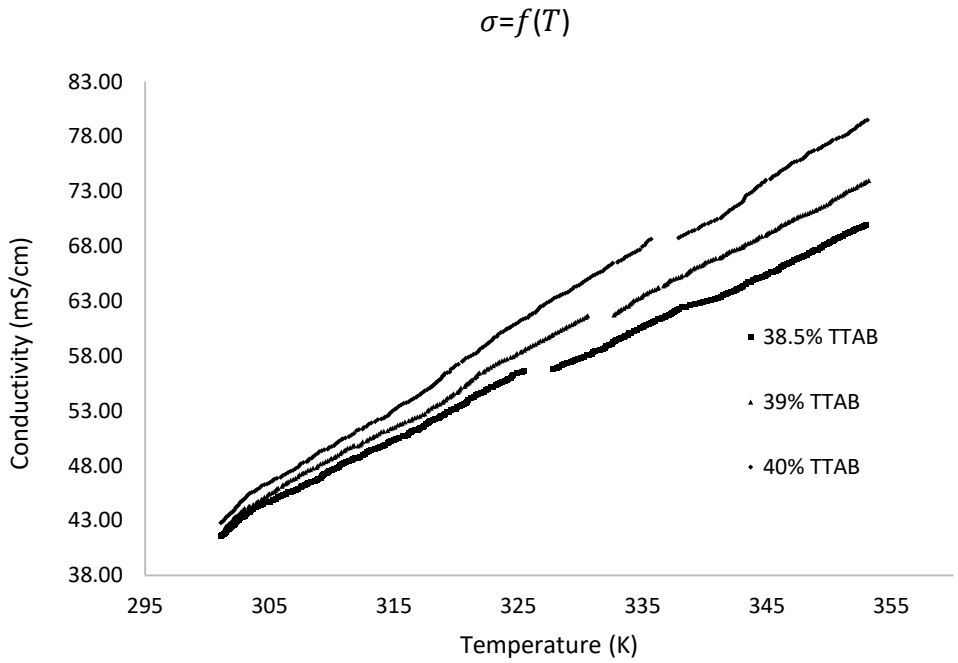

Figure 40: $\sigma = f(T)$ dependences for N_C mesophase. (Samples with 38.5 $wt\%$ TTAB + 61.5 $wt\%$ salty water, 39 $wt\%$ TTAB + 61 $wt\%$ salty water and 40 $wt\%$ TTAB + 60 $wt\%$ salty water compositions)

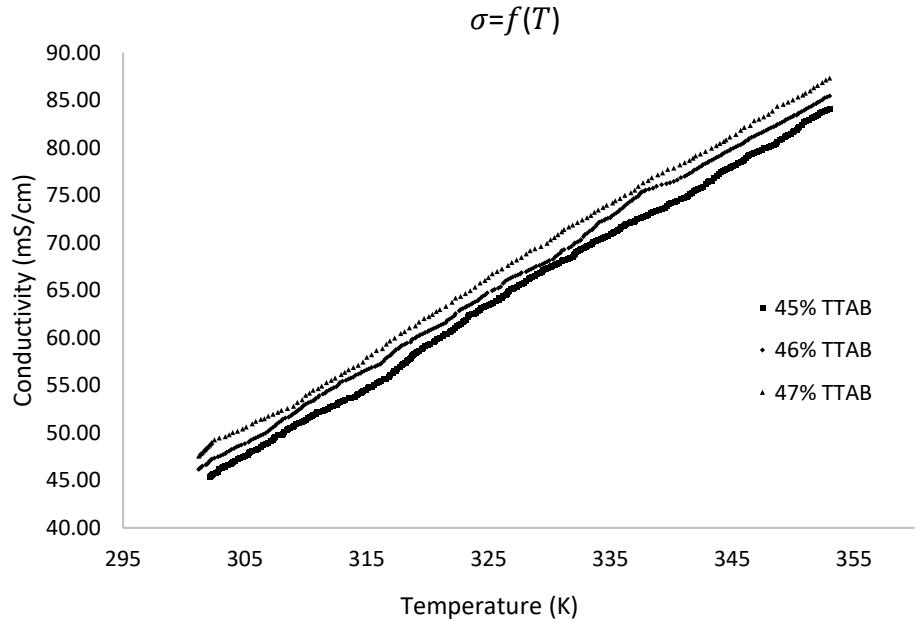

Figure 41: $\sigma = f(T)$ dependences for E mesophase. (Samples with 45 $wt\%$ TTAB + 55 $wt\%$ salty water, 46 $wt\%$ TTAB + 54 $wt\%$ salty water and 47 $wt\%$ TTAB + 53 $wt\%$ salty water compositions)

Comparing the temperatures at which the anomalies begin to appear in the $n = f(T)$ and $\sigma = f(T)$ dependences, they are equal for samples with same compositions, and they match with the thermotropic phase transition temperatures obtained in POM investigations, given in Table 2, as in BLS.

Table 2: Thermotropic phase transition temperatures obtained by different methods; POM, $n = f(T)$ dependences and $\rho = f(T)$ dependences.

TTAB concentration	**phase/mesophase**	**phase transition temperature obtained from POM**	**anomaly temperature on $n = f(T)$ dependence**	**anomaly temperature on $n = f(T)$ dependence**	**corresponding thermotropic phase transition**
35 $wt\%$	L_1	-	-	-	-
36 $wt\%$	L_1	-	-	-	-
37 $wt\%$	L_1	-	-	-	-
38.5 $wt\%$	N_C	321.6 K	321.6 K	321 K	$N_C - L_1$
39 $wt\%$	N_C	325.6 K	325.6 K	325 K	$N_C - L_1$
40 $wt\%$	N_C	330.7 K	330.6 K	330 K	$N_C - L_1$
45 $wt\%$	E	Over 373 K	Over 373 K	Over 373 K	$E - L_1$
46 $wt\%$	E	Over 373 K	Over 373 K	Over 373 K	$E - L_1$
47 $wt\%$	E	Over 373 K	Over 373 K	Over 373 K	$E - L_1$

Figures 42 and 43 represent the $n = f(T)$ dependences and $\sigma = f(T)$ dependences for TTAB + Salty Water TLS respectively.

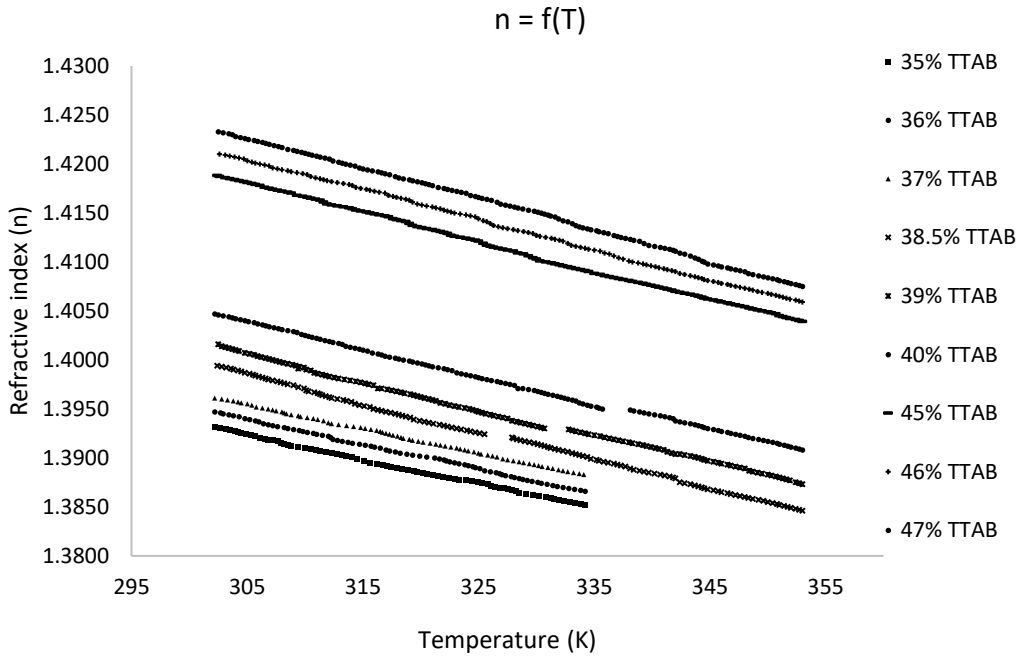

Figure 42: $n = f(T)$ dependences for TTAB + water + NaBr TLS

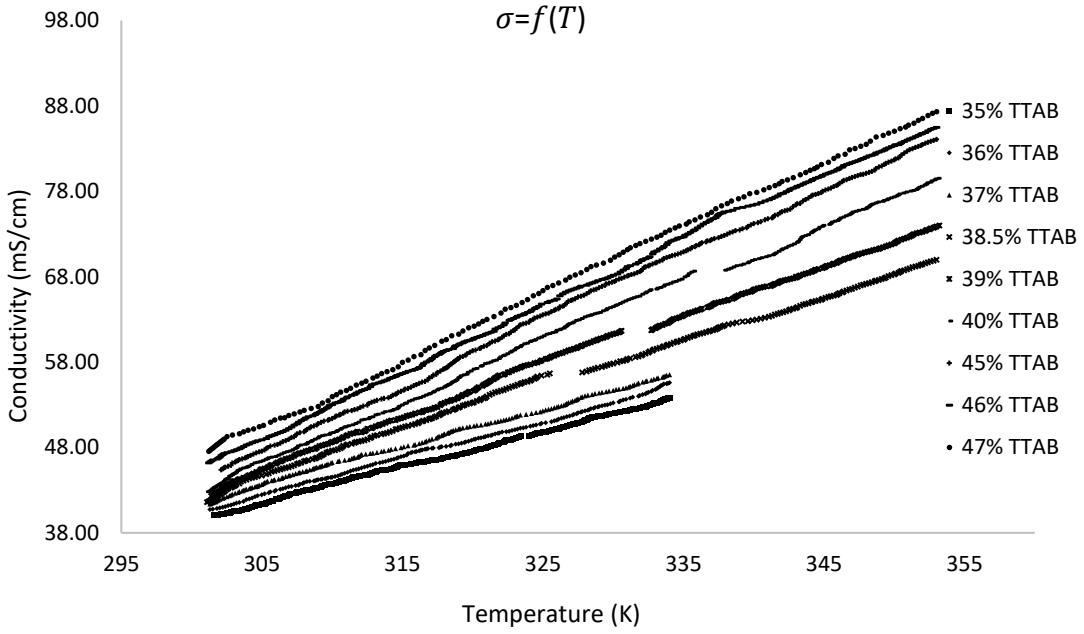

Figure 43: $\sigma = f(T)$ dependences for TTAB + water + NaBr TLS

3.3 Discussion on the Effect of Salt

Inorganic salt addition had a significant influence both on the phase states and physical properties of the binary system. Figure 44 shows the two constructed phase diagrams combined. When analyzed, salt addition shifted the mesophase intervals, increased the phase transition temperatures and changed the width of the mesophase regions. TTAB + Water BLS displayed N_C mesophase in the $37.5 - 38.8\ wt\%$ TTAB concentration interval. This interval has significantly expanded to $38.4 - 41.2\ wt\%$ TTAB concentration with the addition of inorganic salt. Moreover, the addition of salt has increased the polymorphism of the system. N_D mesophase, which does to exist in the BLS, is defined to form in 41.9 – 43.2 wt% TTAB concentration interval with the addition of salt.

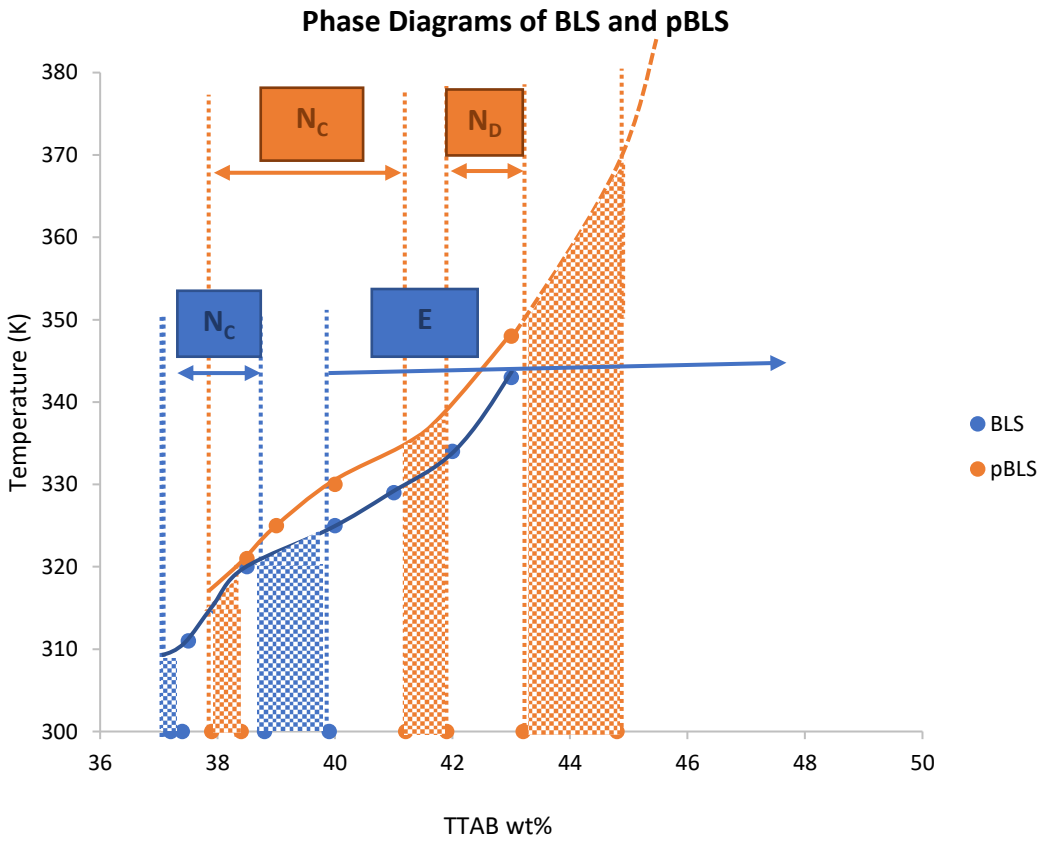

Figure 44: The constructed phase diagrams of BLS and pBLS combined

Figures 45, 46 and 47 represent the $n = f(T)$ and Figures 48, 49 and 50 represent the $\sigma = f(T)$ dependences of the two systems together for the samples with same TTAB concentrations, corresponding to L_1 phase, N_C mesophase and E mesophase respectively. When the given dependences are analyzed, the addition of inorganic salt significantly raised both RI and electroconductivity values for all amphiphile concentrations for all phases/mesophases. Moreover, it raised the amount of increase of the refractive index and electroconductivity values by concentration while it did not affect the change rate by temperature.

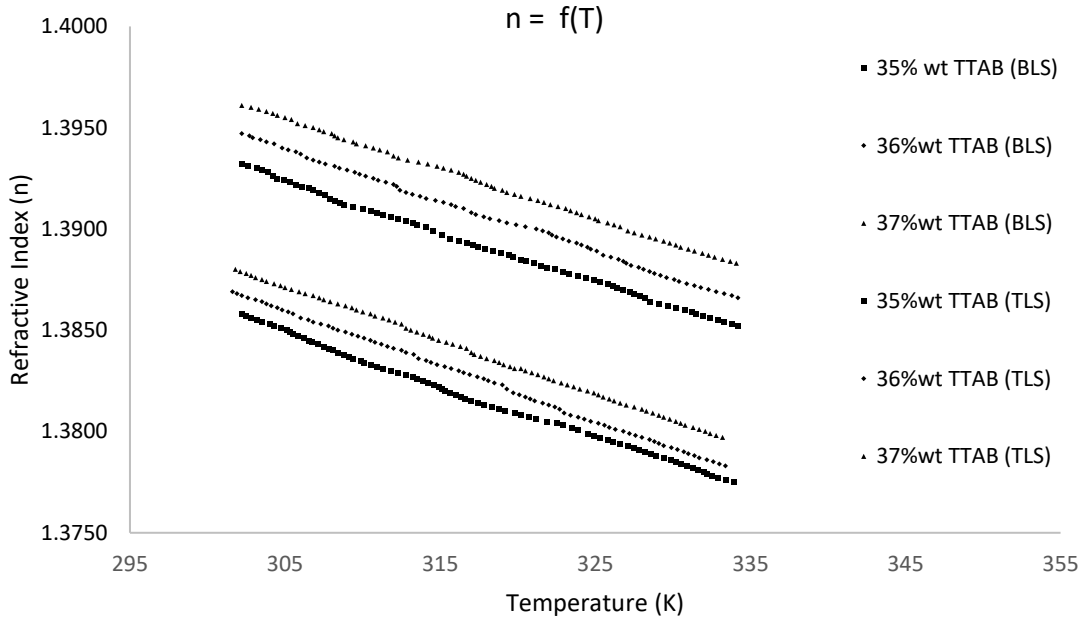

Figure 45: $n = f(T)$ dependences for L_1 phase corresponding to the same TTAB concentrations in two systems combined

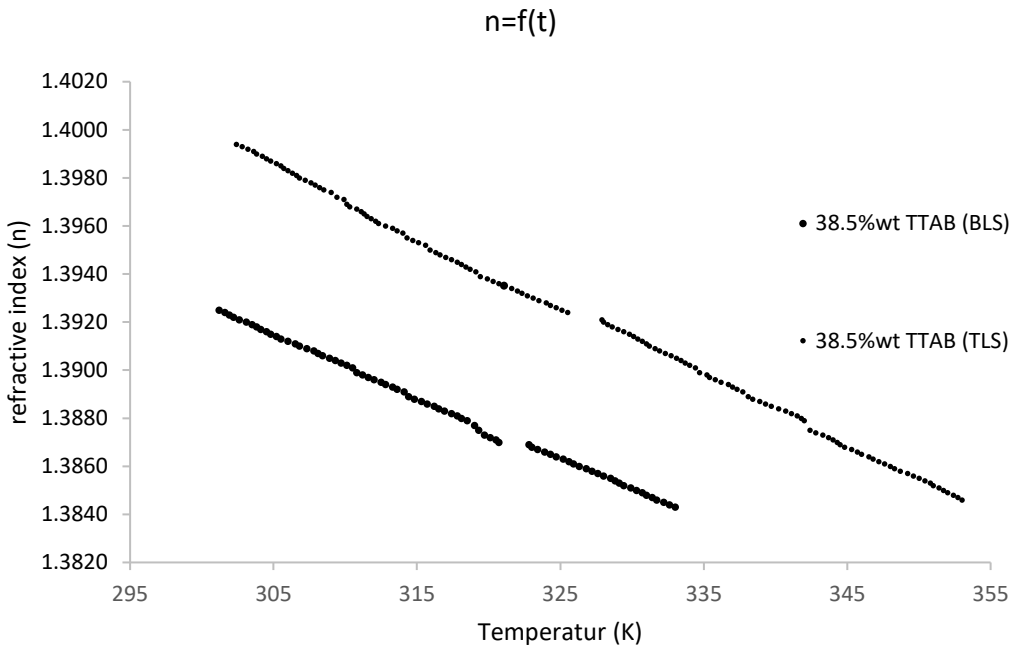

Figure 46: $n = f(T)$ dependences for N_C mesophase corresponding to the same TTAB concentration in two systems combined

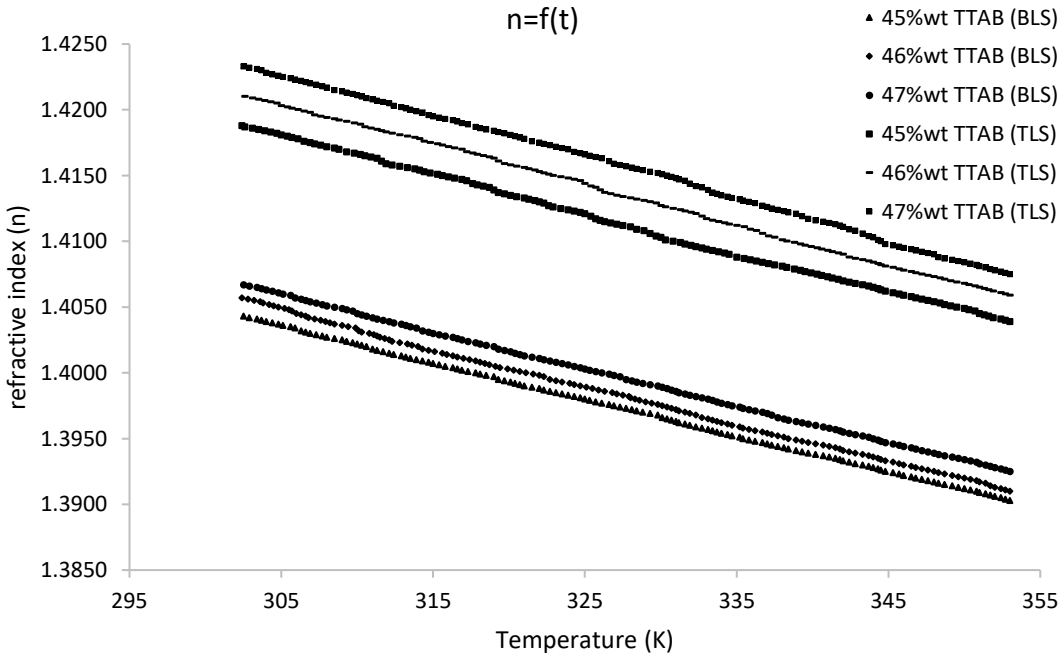

Figure 47: $n = f(T)$ dependences for E mesophase corresponding to the same TTAB concentrations in two systems combined

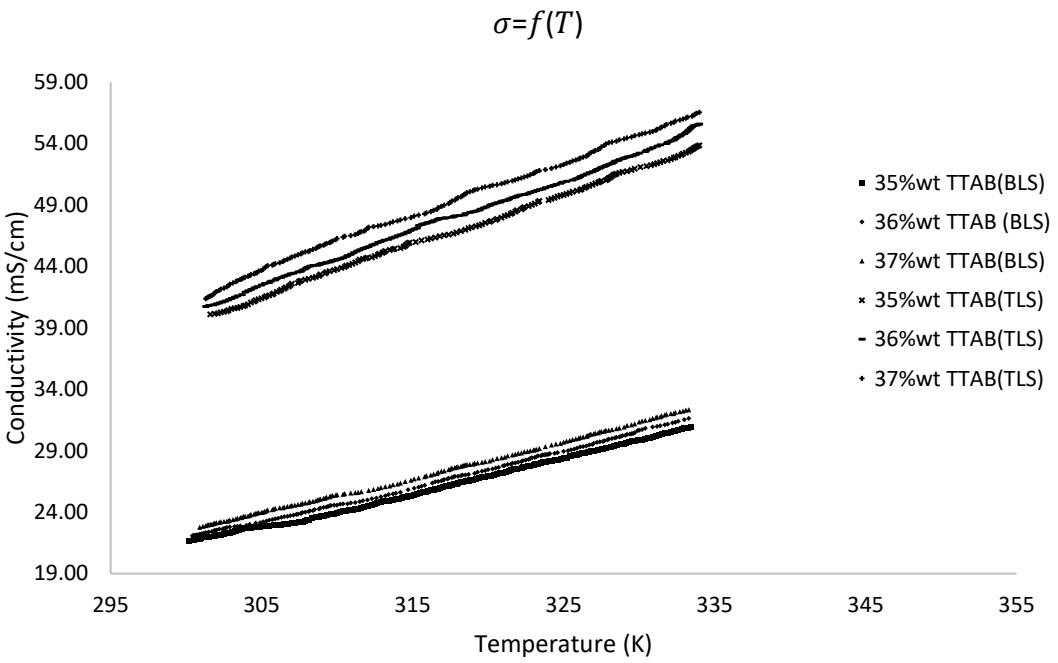

Figure 48: $\sigma = f(T)$ dependences for L_1 phase corresponding to the same TTAB concentrations in two systems combined

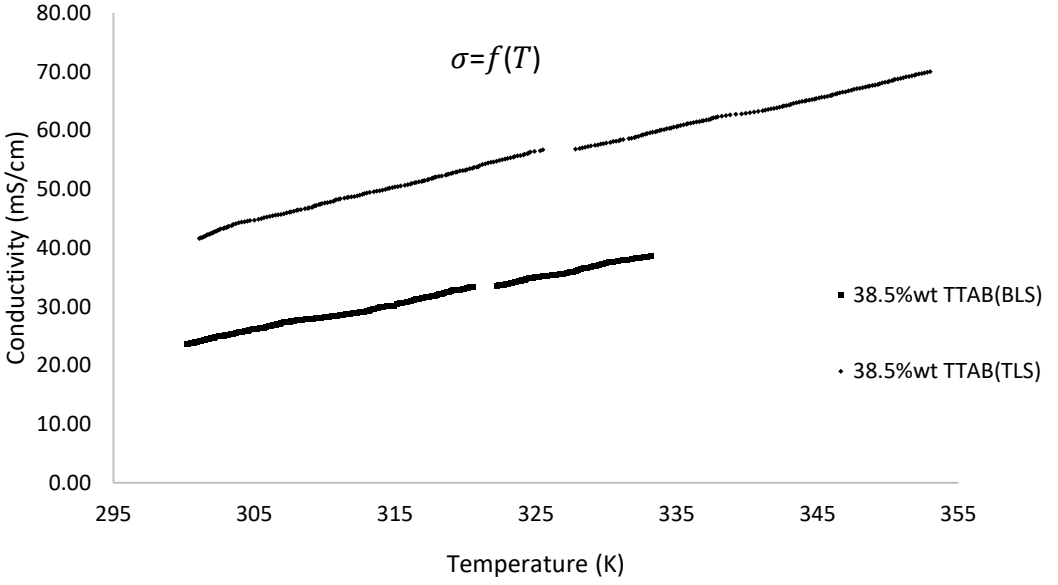

Figure 49: $\sigma = f(T)$ dependences for N_C mesophase corresponding to the same TTAB concentration in two systems combined

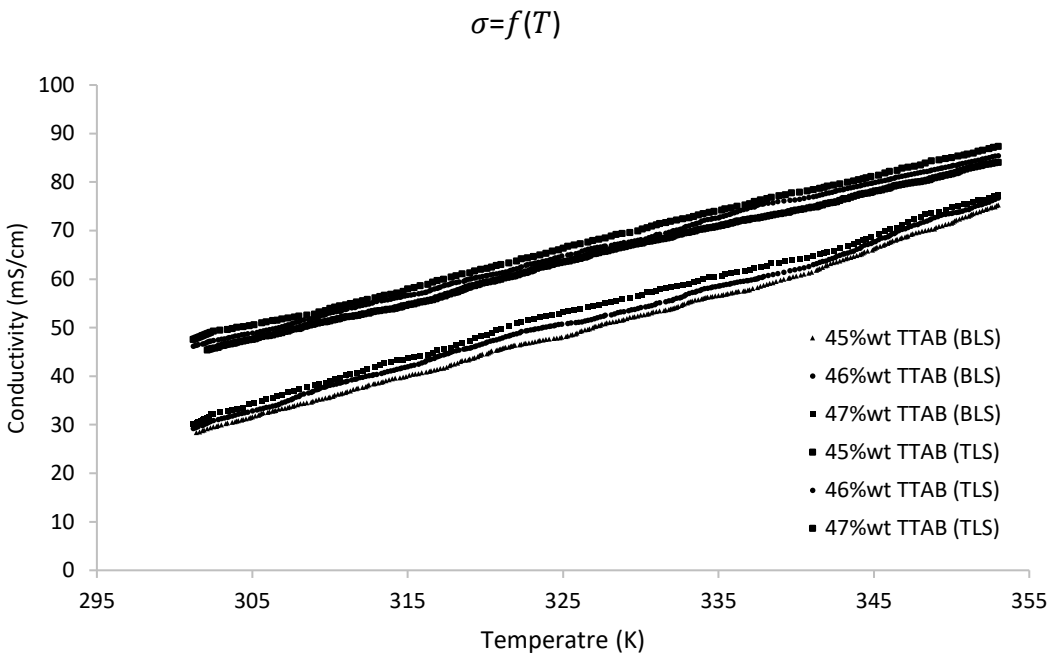

Figure 50: $\sigma = f(T)$ dependences for E mesophase corresponding to the same TTAB concentrations in two systems combined

Chapter 4

CONCLUSION

It is known from the literature [34] that measuring the physical parameters and analysing their temperature and concentration dependences is a sufficiently successful method to define the thermotropic and lyotropic phase transitions. Likewise, it is the general case that all the mesophases displayed by a binary system form again when a co surfactant is added to it [47, 50]. The results obtained in this study are in line with those literature.

On the other side, although there are some studies referring to the effect of salt on some properties of different LLC systems partially [54-58], there is not any extensive study discussing the effect of salt on the phase states, refractive index and electroconductivity values, and the dependences of those values on temperature and concentration. These facts make the following conclusions reached important results for literature.

The addition of salt shifted thermotropic and lyotropic phase transitions, side by side widening the nematic calamitic mesophase region. Furthermore, nematic discotic mesophase that was not observed in the binary system, formed. Those results clearly implies that addition of salt on a binary system has significant effects on its phase states and polymorphism.

The addition of salt has significantly increased the refractive index values and raised the amount of increase with the increase in amphiphile concentration for all mesophases. Likewise, the addition of salt has significantly increased the conductivity values and raised the amount of increase with the increase in amphiphile concentration for L_1 phase, whereas it did it for mesophases.

REFERENCES

[1] Timothy J. Sluction, Daavid A. Dunmur and Horst Stegemeyer (2004). *Crystals That Flow*, C1, 3– 24.

[2] Reintizer, F. (1888). Beiträge zur Kenntniss des Cholesterins. *Monatshefte für Chemie - Chemical Monthly*, *9*(1), 421–441.

[3] Lehmann, O. (1890). Ueber Tropfbarflüssige Krystalle. *Annalen Der Physik Und Chemie*, *276*(7), 401–423.

[4] Gattermann, L. and Ritschke, A. (1890). Ueber Azoxyphenoläther. *Berichte Der Deutschen Chemischen Gesellschaft*, *23*(1), 1738–1750.

[5] Meyer, F.and Dahlem, K. (1903). Azo- und Azoxybenzoäureester, *Ann. Chemie 331*, 331 – 346.

[6] Vorländer (1907). Neue Erscheinungen beim Schmelzen und Krystallisieren, *Z. Physik. Chem. 57*, 357.

[7] Friedel, G. (1922). Les États Mésomorphes De La Matière. *Annales De Physique*, *9*(18), 273–474.

[8] Oseen, C.W. (1923) Versuch einer kinetischen Theorie der kristallinischen Flüssigkeiten, III Abhandlung. (Essay on a kinetic theory of crystalline fluids, part 3.) *Kungligar Svenska Vetenskapakademiens Handligar 63*(12).

[9] Oseen, C.W. (1929) Die anisotropen Flüssigkeiten. Tatsachen und Theorien. (Anisotropic liquids: experiments and theories.) *Fortschritte der Chemie, Physik und Physikalischer Chemie 20*(2) Berlin.

[10] Oseen, C.W. (1933) The theory of liquid crystals. *Transactions of the Faraday Society 29*, 883–900

[11] Maier, W. and Saupe, A. (1958). Eine Einfache Molekulare Theorie Des Nematischen Kristallinflüssigen Zustandes. *Zeitschrift Für Naturforschung a*, *13*(7), 564–566.

[12] Kelker, H.and Scheurle, B. (1969). A Liquid Crystalline (Nematic) Phase with a Particularly Low Solidification Point, *Angewandte Chemi*, *8*(11), 884-885.

[13] Schadt, M. (2017). Liquid Crystal displays, LC-materials and LPP photo-alignment. *Molecular Crystals and Liquid Crystals*, *647*(1), 253–268.

[14] Heilmeier, G.H. and Zanoni, L.A. (1968). Guest-Host Interactions In Nematic Liquid Crystals. A New Electro-Optic Effect. *Applied Physics Letters, 13*(3), 91–92.

[15] Saupe, A. (1969). On Molecular Structure and Physical Properties of Thermotropic Liquid Crystals. *Molecular Crystals*, *7*(1), 59–74.

[16] Schadt, M. And Helfrich, W. (1971). Voltage-Dependent Optical Activity Of A Twisted Nematic Liquid Crystal. *Applied Physics Letters*, *18*(4), 127–128.

[17] Meyer, R.J. and McMillan, W.L. (1974). Simple Molecular Theory of the Smectic C,B, and H Phases. *Physical Review a*, *9*(2), 899–906.

[18] Cladis, P.E. (1975). New Liquid-Crystal Phase Diagram. *Physical Review Letters*, *35*(1), 48–51.

[19] Meyer, R.B. (1977). Ferroelectric Liquid Crystals; a Review. *Molecular Crystals and Liquid Crystals*, *40*(1), 33–48.

[20] Chandrasekhar, S. and Litster, J.D. (1978). Liquid Crystals. *Physics Today*, *31*(4), 55–56.

[21] Yu, L.J. and Saupe, A. (1980). Observation of a Biaxial Nematic Phase in Potassium Laurate-1-Decanol-Water Mixtures. *Physical Review Letters*, *45*(12), 1000–1003.

[22] Crane, H.R. (1983). Liquid Crystal displays: watches, Calculators and (soon) Cars. *The Physics Teacher*, *21*(7), 467–467.

[23] Rajak, P., Nath, L.K. and Bhuyan, B. (2019). Liquid Crystals: an Approach in Drug Delivery. *Indian Journal of Pharmaceutical Sciences*, *81*(1).

[24] Castellano, J.A. (1991). Liquid Crystal Display Applications: Past, Present & Future. *Liquid Crystals Today*, *1*(1), 4–6.

[25] Darrel D. Ebbing and Steven D. Gammon (2007), *General Chemistry,* Houghton Mifflin Company, Boston – New York, nineth edition.

[26] Atkins P. and de Paula J., (2010), *Physical Chemistry*, Oxford University Press, nineth edition.

[27] Shri Singh and Dunmur, D.A. (2002). *Liquid Crystals : Fundamentals*. Singapore ; River Edge: World Scientific.

[28] Figueiredo, A. M. Neto and Sílvio, R. A. Salinas (2005). *The Physics of Lyotropic Liquid Crystals* : *Phase Transitions and Structural Properties*. New York: Oxford University Press.

[29] David J.R. Cristaldi, Salvadore Pennissi and Francesco Pulvirenti (2009), *Liquid Crystal Display Drivers*, Springer.

[30] Ingo Dierking (2003), *Textures of Liquid Crystals*, Willey-VCH Verlag.

[31] Vertogen, G., De Jeu, W. H. *Thermotropic Liquid Crystals; Fundamentals*, Springer Verlag, 1987.

[32] Ki Kicheff, C. Grabielle Madelmont, And M. Ollivon (1988), Phase Diagram of Sodium Dodecyl Sulfate – Water System, *Journal of Colloid and Interface Science, v. 131*, 112-132.

[33] Camillo La Mesa, Bianca Sesta, Maria Grazia Bonicelli and Gian Franco Ceccaroni (1990), Phase Diagram of the Binary System Water (Dodecyl dimethyl ammonium) propane sulfonate, *Langmuirr, v. 6,* 728-731.

[34] Masalci, Ö., Okcan, M., Kazanci, N. (2007), Refracting and Electrical Properties and The Phase Equilibria of The TTAB + Water Binary System (2007), *Journal of Molecular Structure, v. 843,* 32-37.

[35] Antara Pal, Rose Marry, V.A. Raghunathan (2012), Phase Behavior of The Cetyltrimethylammonium Tosylate (CTAT)–Water System, *Journal of Molecular Liquids, V. 174,* 48-51.

[36] Shinichi Yano, Kenji Tadano, Koichiro Aoki (2014), Studies of Lyotropic Liquid Crystalline Phase in Sodium Decylsulfate - Water System by Density and Conductivity Measurements, *Molecular Crystals and Liquid Crystals, V. 92,* 99-104.

[37] Brian Cull, M. Heino, S. H. Lee, Satyendra Kumar, S. S. Keast and M. E. Neubert (2015), Effect of salt on the phase diagrams of two binary lyotropic liquid crystalline solutions, *Liquid Crystals, v. 17,* 507-512.

[38] Sadaf Sarfnaz, Shahid Ali, Safyan Akram Khan, Khizar Hussain Shah, Shahid Amin, Mohammad Mujahid, Saba Jamil, Muhammad Ramzeh Saeed, and Ashraf Janjua (2017), Phase Diagram and Surface Adsorption Behaviour of Benzyl Dimethyl Hexadecyl Ammonium Bromide in a Binary Surfactant-Water System, *Journal of Molecular Liquids, v. 285,* 403-407.

[39] Taro Yamamoto, Yusuke Yagi, Toshimitsu Hatakeyama, Tomonari Wakanayashi, Tadashi Kamiyama and Hal Suzuki (2021), Metastable and stable phase diagrams and thermodynamic properties of the cetyltrimethylammonium bromide (CTAB)/water binary system, *Colloids and Surfaces A, v. 625*, 126859.

[40] Yıldız, T., Kazanci, N. (2008), Investigation of temperature dependence of mesomorphism and refracting index of sodium dodecylsulphate + water + Decanol lyotropic system, *Journal of Molecular Structure, v. 886*, 158-165.

[41] Meier, G., Sackmann, E., Grabmaier, J.G. (1975), *Applications of Liquid Crystals*, Springer -Verlag.

[42] Jakli, A., Saupe, A. (2006), *One- and Two- Dimensional Fluids*, Taylor & Francis.

[43] Richard A. Paselk (2004), *The Evolution of the Abbe Refractometer*, Nuncius, v. 19, pp. 19-22.

[44] Richard A. Paselk (1999), *The Chemical Refractometer*, v. 62, pp. 725-732.

[45] Emerson (2010), *Theory And Application Of Conductivity*, ADS 43-018/rev.D.

[46] Shri Singh (foreword by David A. Dunmur) (2002), *Liquid Crystals*, World Scientific.

[47] Nesrullajev, A., Okcan, M., Kazanci, N. (2003), Comperative Peculiarities of Non-uniform Textures of Lyotropic Mesophases of Binary and Ternary Systems Based on n-cetyl-n,n,n-timethyl ammonium bromide, *Journal of molecular liquids, v. 108/1-3,* 313-332.

[48] Nesrullajev, A., Kazanci N. (2000), Lyotropic Nematic Mesophases: Investigations of Mesomorphic and Thermo-Optical Properties, *Materials Chemistry and Physics, v. 62,* 230-235.

[49] Yıldız, T., Kazancı N. (2008), Investigation of Temperature Dependence of Mesomorphism and Refractive Index of Sodium Dodecyl Sulphate + Water + Decanol Lyotropic System, *Journal of Molecular Structure, v. 886,* 158-165.

[50] Masalcı, Ö., Kazanci N. (2009), Compared Properties of Textures of Lyotropic Mesophases of Binary and Ternary Sytems Based on Tetradecyltrimethyl Ammonium Bromide, *Journal of Molecular Structure, v. 919,* 1-6.

[51] Yavuz, A. E. Masalci, Ö., Kazancı N. (2014), Phase Diagram of Tetradecyltrimethylammonium Bromide (TTAB) + Water + Octanol System with Application of Mechanical Deformation, *Applied Surface Science, v. 318,* 251-255.

[52] Kazancı, N., Nesrullajev A. (2002), Refracting and Birefringent Properties of Lyotropic Nematic Mesophases, *Materials Research Bulletin, v. 38,* 1003-1012.

[53] Krishna, S. Prasad, K. L. Sandhya, Geetha G. Nair, Uma S. Hiremath, C. V. Yelamaggad and S. Sampath (2006), Electrical conductivity and dielectric constant measurements of liquid crystal–gold nanoparticle composites, *Liquid Crystals, v. 33,* 1121-1125.

[54] De Melo Filho, A.A., Amadeu, N.S. and Fujiwara, F.Y. (2007). The Phase Diagram of the Lyotropic Nematic Mesophase in the TTAB/NaBr/water System. *Liquid Crystals*, *34*(6), 683–691.

[55] Nishio, Y., Chiba, R., Miyashita, Y., Oshima, K., Miyajima, T., Kimura, N. and Suzuki, H. (2002). Salt Addition Effects on Mesophase Structure and Optical Properties of Aqueous Hydroxypropyl Cellulose Solutions. *Polymer Journal*, *34*(3), 149–157.

[56] Maiti, K., Mitra, D., Guha, S. and Moulik, S.P. (2009). Salt Effect on self-aggregation of Sodium Dodecylsulfate (SDS) and Tetradecyltrimethylammonium Bromide (TTAB): Physicochemical Correlation and Assessment in the Light of Hofmeister (lyotropic) Effect. *Journal of Molecular Liquids*, 146(1-2), pp.44–51.

[57] Nesrullajev, A., Kazanci, N. (1998). Effect of the inorganic salt on the electrical conductivity characteristics of lyotropic nematic. *Czech J Phys 48*, 1607–1613

[58] Masalci, O., Kazanci, N., Orujalipoor, I. and İde, S. (2015). Nano-Structural Analysis of a Lyotropic Liquid Crystal (TTAB + Water + Decanol ternary) System by Salt (NH4Br) Addition. *Molecular Crystals and Liquid Crystals*, *609*(1), 70–79.